SYSTEM-LEVEL SIMULATION OF A THIRD GENERATION WCDMA WIRELESS GEOLOCATION NETWORK

by
SANEM KABADAYI

Submitted to the Graduate School of Engineering and Natural Sciences
in partial fulfillment of
the requirements for the degree of
Master of Science
in
Electrical Engineering

Sabancı University
July 2002

SYSTEM-LEVEL SIMULATION OF A THIRD GENERATION WCDMA WIRELESS GEOLOCATION NETWORK

APPROVED BY:

Dr. İbrahim Tekin …….
(Thesis Supervisor)

Dr. Ayhan Bozkurt …….

Dr. Ahmet Onat …….

DATE OF APPROVAL: …….

To the memory of Mustafa Kemal Atatürk
who made it possible for me to pursue a career in science
and
to my mother, Müjde,
my father, Ülkü,
my brother, Kerem,
my grandmother, Semiha

ACKNOWLEDGMENTS

I would like to thank my thesis supervisor, Dr. İbrahim Tekin, for his guidance, valuable suggestions, answering my seemingly endless questions, and for being at Sabancı University when I arrived. I am grateful to Dr. Ece Saygun for initiating me to the world of GSM and for her friendship.

I am thankful to Melis Ekinci and Tugba Demirci for their friendship and support.

I am forever grateful to my family for their unconditional love and support. I cannot thank my parents enough for giving me the best of everything in the world, for all their sacrifices, and everything they have taught me. In addition, I thank my mother for staying up with me on countless nights and my father for contributing his laptop to the massive simulation effort at home.

SYSTEM-LEVEL SIMULATION OF A THIRD GENERATION WCDMA WIRELESS GEOLOCATION NETWORK

ABSTRACT

A wireless geolocation system for use in a WCDMA (Wideband Code Division Multiple Access) network was simulated in Matlab. In such a system, the multipath delays have a significant effect on the mobile location estimate.

First, the path loss, shadowing, and fading models were analyzed for a 19-cell 3-sector topology with a 5-km cell radius, using lognormal shadowing with a standard deviation of 8 dB. Then, a Simulink end-to-end model was created according to WCDMA system specifications, where the pilot signal was spread using 38400-chip complex Gold spreading and shaped using a square-root raised cosine transmit filter. The effects of multipath fading and noise were added.

At the receiver, the received signal was passed through a receive filter and correlated with the mobile station's locally generated Gold code. The delay in the peaks of the correlator determined which multipath delay was taken to be the distance from the base station. The geolocation system implemented in Matlab estimated the mobile location using the delay added propagation times. The hyperbolic time-difference-of-arrival approach was employed for forming an estimate of the mobile station.

The estimation error was calculated for the COST-231 suburban, urban, and rural environments using CODIT, ATDMA, ITU Vehicular A, and ITU Vehicular B channel models. This error was found to be less than 20 m for the suburban ATDMA model and less than 110 m for the rural CODIT model 90% of the time. The estimation errors ranged between these values for the other combinations. These errors are acceptable considering that one chip time corresponds to 78 m. Also, for comparison, the former WCDMA specification of 40960-chip complex spreading was evaluated and in this case the error was found to be less than 100 m 90% of the time for the COST-231 suburban

model using the CODIT Macro Channel. In this case, one chip time corresponds to 73 m.

This system does not require network synchronization and was found to be an acceptable geolocation system for WCDMA under the given conditions.

SYSTEM-LEVEL SIMULATION OF A THIRD GENERATION WCDMA WIRELESS GEOLOCATION NETWORK

ÖZET

Geniş bantlı CDMA ağlarında kullanılmak üzere, Matlab ve Simulink'te bir coğrafi yer saptama sisteminin simülasyonu yapıldı. Böyle bir sistemde, çeşitli yollar takip eden sinyalin gecikmesinin gezgin istasyon yerinin tahmininde büyük bir etkisi vardır.

Öncelikle, 19 hücreli, 3 bölgeli, ve hücre yarıçapı 5 km olan bir topoloji için 8 dB standart sapmalı bir lognormal gölgeleme modeli kullanılarak yol kaybı, gölgeleme ve solma incelendi. Daha sonra, geniş bantlı CDMA sistem tarifine uygun olarak pilot sinyalin 40960 çiplik compleks Gold koduyla yayıldığı ve karekök üslü kosinüs filtresinden geçirilerek şekillendirildiği bir Simulink modeli yaratıldı. Çeşitli yolların yarattığı sinyal solmasının ve gürültünün etkisi de eklendi.

Alıcıda, alınan sinyal bir alıcı filtresinden geçirildi ve gezgin istasyonun kendi oluşturduğu Gold koduyla bir anda 80 çipi işleyerek 480 zaman çerçevesi yaratacak şekilde korele edildi. Korelasyon sonucu elde edilen zirveler baz istasyondan olan uzaklığa eklenen çeşitli yola bağlı olan gecikmeyi belirledi. Matlab'de yaratılan coğrafi yer saptama sistemi, bu gecikme eklenmiş uzaklıkları kullanarak gezgin istasyonun yer tahminini yaptı. Bu tahmini oluşturmak için hiperbolik gelişteki zaman farkı tekniği kullanıldı.

Konum tahmininde yapılan hata, COST-231 banliyö, şehir ve kırsal modelleri için CODIT, ATDMA, ITU Vehicular A ve ITU Vehicular B kanal modelleri kullanılarak hesaplandı. Banliyö ATDMA modeli için bu hatanın %90 olasılıkla 20m'den az, kırsal CODIT modeli içinse 110m'den az olduğu bulundu. Diğer modeler için bulunan hataların bu iki değer arasında değiştiği görüldü. Bir çip zamanının 78 metreye denk geldiği düşünülürse, bu kabul edilebilir bir hatadır. Karşılaştırma amaçlı olarak, 40960 çiplik, bir çip zamanının 73 metreye denk geldiği eski WCDMA tarifi de COST-231 banliyö modeli için CODIT kullanılarak değerlendirildi ve hatanın %90 olasılıkla 100m'den az olduğu bulundu.

Senkronizasyon gerektirmeyen bu sistem, söz konusu şartlar altında geniş bantlı CDMA için uygun bir coğrafi yer saptama sistemidir.

TABLE OF CONTENTS

TABLE OF CONTENTS (continued)

LIST OF TABLES

LIST OF FIGURES

LIST OF FIGURES (continued)

SYSTEM-LEVEL SIMULATION OF A THIRD GENERATION WCDMA WIRELESS GEOLOCATION NETWORK

by
SANEM KABADAYI

Submitted to the Graduate School of Engineering and Natural Sciences
in partial fulfillment of
the requirements for the degree of
Master of Science
in
Electrical Engineering

Sabancı University
July 2002

SYSTEM-LEVEL SIMULATION OF A THIRD GENERATION WCDMA WIRELESS GEOLOCATION NETWORK

APPROVED BY:

Dr. İbrahim Tekin …….
(Thesis Supervisor)

Dr. Ayhan Bozkurt …….

Dr. Ahmet Onat …….

DATE OF APPROVAL: …….

To the memory of Mustafa Kemal Atatürk
who made it possible for me to pursue a career in science
and
to my mother, Müjde,
my father, Ülkü,
my brother, Kerem,
my grandmother, Semiha

ACKNOWLEDGMENTS

I would like to thank my thesis supervisor, Dr. İbrahim Tekin, for his guidance, valuable suggestions, answering my seemingly endless questions, and for being at Sabancı University when I arrived. I am grateful to Dr. Ece Saygun for initiating me to the world of GSM and for her friendship.

I am thankful to Melis Ekinci and Tugba Demirci for their friendship and support.

I am forever grateful to my family for their unconditional love and support. I cannot thank my parents enough for giving me the best of everything in the world, for all their sacrifices, and everything they have taught me. In addition, I thank my mother for staying up with me on countless nights and my father for contributing his laptop to the massive simulation effort at home.

SYSTEM-LEVEL SIMULATION OF A THIRD GENERATION WCDMA WIRELESS GEOLOCATION NETWORK

ABSTRACT

A wireless geolocation system for use in a WCDMA (Wideband Code Division Multiple Access) network was simulated in Matlab. In such a system, the multipath delays have a significant effect on the mobile location estimate.

First, the path loss, shadowing, and fading models were analyzed for a 19-cell 3-sector topology with a 5-km cell radius, using lognormal shadowing with a standard deviation of 8 dB. Then, a Simulink end-to-end model was created according to WCDMA system specifications, where the pilot signal was spread using 38400-chip complex Gold spreading and shaped using a square-root raised cosine transmit filter. The effects of multipath fading and noise were added.

At the receiver, the received signal was passed through a receive filter and correlated with the mobile station's locally generated Gold code. The delay in the peaks of the correlator determined which multipath delay was taken to be the distance from the base station. The geolocation system implemented in Matlab estimated the mobile location using the delay added propagation times. The hyperbolic time-difference-of-arrival approach was employed for forming an estimate of the mobile station.

The estimation error was calculated for the COST-231 suburban, urban, and rural environments using CODIT, ATDMA, ITU Vehicular A, and ITU Vehicular B channel models. This error was found to be less than 20 m for the suburban ATDMA model and less than 110 m for the rural CODIT model 90% of the time. The estimation errors ranged between these values for the other combinations. These errors are acceptable considering that one chip time corresponds to 78 m. Also, for comparison, the former WCDMA specification of 40960-chip complex spreading was evaluated and in this case the error was found to be less than 100 m 90% of the time for the COST-231 suburban

model using the CODIT Macro Channel. In this case, one chip time corresponds to 73 m.

This system does not require network synchronization and was found to be an acceptable geolocation system for WCDMA under the given conditions.

SYSTEM-LEVEL SIMULATION OF A THIRD GENERATION WCDMA WIRELESS GEOLOCATION NETWORK

ÖZET

Geniş bantlı CDMA ağlarında kullanılmak üzere, Matlab ve Simulink'te bir coğrafi yer saptama sisteminin simülasyonu yapıldı. Böyle bir sistemde, çeşitli yollar takip eden sinyalin gecikmesinin gezgin istasyon yerinin tahmininde büyük bir etkisi vardır.

Öncelikle, 19 hücreli, 3 bölgeli, ve hücre yarıçapı 5 km olan bir topoloji için 8 dB standart sapmalı bir lognormal gölgeleme modeli kullanılarak yol kaybı, gölgeleme ve solma incelendi. Daha sonra, geniş bantlı CDMA sistem tarifine uygun olarak pilot sinyalin 40960 çiplik compleks Gold koduyla yayıldığı ve karekök üslü kosinüs filtresinden geçirilerek şekillendirildiği bir Simulink modeli yaratıldı. Çeşitli yolların yarattığı sinyal solmasının ve gürültünün etkisi de eklendi.

Alıcıda, alınan sinyal bir alıcı filtresinden geçirildi ve gezgin istasyonun kendi oluşturduğu Gold koduyla bir anda 80 çipi işleyerek 480 zaman çerçevesi yaratacak şekilde korele edildi. Korelasyon sonucu elde edilen zirveler baz istasyondan olan uzaklığa eklenen çeşitli yola bağlı olan gecikmeyi belirledi. Matlab'de yaratılan coğrafi yer saptama sistemi, bu gecikme eklenmiş uzaklıkları kullanarak gezgin istasyonun yer tahminini yaptı. Bu tahmini oluşturmak için hiperbolik gelişteki zaman farkı tekniği kullanıldı.

Konum tahmininde yapılan hata, COST-231 banliyö, şehir ve kırsal modelleri için CODIT, ATDMA, ITU Vehicular A ve ITU Vehicular B kanal modelleri kullanılarak hesaplandı. Banliyö ATDMA modeli için bu hatanın %90 olasılıkla 20m'den az, kırsal CODIT modeli içinse 110m'den az olduğu bulundu. Diğer modeler için bulunan hataların bu iki değer arasında değiştiği görüldü. Bir çip zamanının 78 metreye denk geldiği düşünülürse, bu kabul edilebilir bir hatadır. Karşılaştırma amaçlı olarak, 40960 çiplik, bir çip zamanının 73 metreye denk geldiği eski WCDMA tarifi de COST-231 banliyö modeli için CODIT kullanılarak değerlendirildi ve hatanın %90 olasılıkla 100m'den az olduğu bulundu.

Senkronizasyon gerektirmeyen bu sistem, söz konusu şartlar altında geniş bantlı CDMA için uygun bir coğrafi yer saptama sistemidir.

TABLE OF CONTENTS

TABLE OF CONTENTS (continued)

LIST OF TABLES

LIST OF FIGURES

LIST OF FIGURES (continued)

CHAPTER 1

INTRODUCTION

In this thesis, we will describe and analyze a geolocation system for a third generation WCDMA (Wideband Code Division Multiple Access) network. The aim is to obtain the link (one mobile, one base station) and system (multiple mobiles, multiple base stations) level performance of a wireless geolocation network for UMTS (Universal Mobile Telecommunications System). Mobile location finding lies at the heart of this problem.

The major propelling force behind wireless geolocation network implementations is the need to locate mobile callers requesting emergency assistance from emergency call centers such as 112 in Europe. The increase in cellular phone usage has resulted in an increase in the number of emergency calls originating from cellular phones. In such applications, the location must be accurate to within a few hundred meters and it must be calculated within a few seconds after the initiation of the call.

Mobile station positioning has numerous applications for law enforcement as well. Stolen cellular phones blacklisted in the Equipment Register can be located the minute they are switched on. In the future, the mobile station location might have criminal justice applications such as locating stolen cars, runaway prisoners, wanted suspects, and lost people[1,2].

From the service providers' point of view, position location offers many commercial applications. The service providers can offer additional services such as mobile yellow pages, equipment tracking, location specific advertising, navigation assistance, and zone-based billing[3]. Zone-based billing allows the subscriber to use a mobile phone, but be billed as if it were a fixed phone in the home zone. When used in

the home zone, the mobile station does not use usual mobile phone features such as handoff and roaming. Outside the home zone, however, the user is billed at the normal mobile rate.

Position specific information services are another potential application of mobile station location. The user can obtain information which is specific to the current position. An SMS (short message service) request and response mechanism can be used for asking for the location of the nearest restaurant and getting the directions to that location. Establishing a staffed pay-per-call map service, where an operator can give directions to the user, is possible for current networks. The user might be able to download a map of the surrounding area with the user's position marked in the future[1].

Mobile station location can also be used for statistical purposes. The network providers can keep statistics of cell usage density to aid in the optimization of mobile networks and deploying new networks[1].

There are three technologies for accurate position location: handset-based technologies such as the Global Positioning System (GPS), network-based technologies that exploit the cellular infrastructure to obtain geolocation information, and hybrid solutions that make use of both technologies[4]. The network-based techniques include angle-of-arrival (AOA), time of arrival, and time difference of arrival (TDOA) measurements. All these techniques make use of the signal transmitted by the mobile station. Combining the known locations of the base stations with the signals received at these locations yields a solution for the mobile's position. It is necessary to know the typical received signal levels and the distribution of these levels in a cellular network. These levels depend on path loss, shadowing, and fading.

This thesis evaluates the TDOA method of estimating the mobile station location in a WCDMA system. Specifically, the effect of multipath propagation on the accuracy of location estimates is observed. The mobile station makes signal arrival-time measurements for the signal from each of the three base stations. In addition, the mobile station is locked onto one base station and at the request of this base station, the mobile station sends a response to all three base stations, resulting in a round-trip measurement at each base station. By processing all these measurements, an estimate for each propagation time can be obtained.

In the absence of multipath fading and noise, this estimate is the actual propagation time. The difference in the arrival times from two base stations defines a

hyperbola with the two stations as the foci. The mobile station lies on this hyperbola. Using another pair of base stations defines another hyperbola and the intersection of these two hyperbolas yields exactly one solution for the mobile position. Multipath fading and noise introduce errors to this location estimate.

In a synchronous network, the clocks of all base stations are synchronized and each base station transmits its pseudonoise sequence at the same time. This synchronization could be accomplished using a common clock source such as GPS.

On the other hand, in an asynchronous network, each base station has an independent reference time and the mobile station does not have prior knowledge of the relative time difference between various base stations. The need to synchronize the base stations to an accurate external timing source is eliminated, making asynchronous operation advantageous in deep in-building coverage or underground deployments.

All base stations continually transmit the continuous common pilot (CPICH) in WCDMA networks. This pilot signal is used by the mobile station to perform searching and identification, in addition to channel tracking and channel estimation[5]. Therefore, time difference of arrival algorithms are readily applicable to WCDMA networks, where the relative arrival times of three or more pilot signals received from different base stations can be used for the location estimation[3].

In WCDMA, the base stations spread the transmitted signal using complex Gold codes in the forward link. By correlating the received signal with its locally generated Gold code, the mobile station can find the delay between the received signal and the original code. This delay is used in finding the mobile's position.

In the simulations, a 3-sector hexagonal cell topology with three directional antennas at the base station is used. The path loss model used in evaluating the downlink performance is the COST-231 model and the fading is modeled using Rayleigh fading. The geolocation system is implemented using the time-difference-of-arrival method.

In the following chapters, the theory behind a WCDMA geolocation network is explained. Then, the simulation procedures are given in the order they were conducted. Finally, the results obtained from the simulations are given.

More specifically, Chapter 2 gives an overview of the theory behind propagation models, WCDMA, spread spectrum, and geolocation. Chapter 3 is a description of the path loss evaluation models, the downlink simulator, and the geolocation system

implemented using Matlab and Simulink. The results and calculations are presented in Chapter 4 along with an analysis of performance. Chapter 5 consists of conclusions and future work.

CHAPTER 2

THEORY

This chapter describes the concepts behind a WCDMA geolocation system. First, the UMTS system is briefly described. Then, general transmission problems such as path loss, shadowing, and fast fading are explained. An overview of different geolocation techniques and direct sequence spread spectrum is given.

2.1. UMTS

GSM (Global System for Mobile Communications) handles voice telephony, facsimile, and electronic mail, but cannot support wideband applications like video, multimedia or high-speed Internet access. This shortcoming of GSM led to the development of a third-generation system, which aims to provide capabilities close to that of fixed networks. In addition to the usual services, provision is made for high-speed Internet access, video telephony and conferencing, entertainment services, and online banking and shopping[6]. To this end, the Universal Mobile Telecommunications System (UMTS) was standardized by ETSI (European Telecommunications Standards Institute).

The ETSI/ARIB WCDMA (Wideband Code Division Multiple Access) proposal, now known as UTRA FDD (Universal Terrestrial Radio Access - Frequency Division Duplex), is asynchronous and serves as the radio interface of UMTS. It is now being developed by the 3GPP (Third Generation Partnership Project). Since the core network

is based on the GSM MAP core network, it is an attractive choice for current GSM operators[7].

Depending upon the user's current environment, the maximum target user bit rates that the UTRA should support are[8]:

- Rural outdoor: 384 kbit/s, maximum mobile speed 500 km/h
- Suburban outdoor: 512 kbit/s, maximum mobile speed 120 km/h
- Indoor/low range outdoor: 2 Mbit/s, maximum mobile speed 10 km/h

2.2. Propagation in a Mobile Radio Environment

In a mobile radio environment, the received signal strength depends on the distance between the transmitter and the receiver and the reflection, diffraction, and scattering due to natural or man-made structures. The variation in the signal strength is described by the superposition of the following effects[9]:

- Path loss
- Shadowing
- Multipath Rayleigh fading

2.2.1. Path Loss Models

The received signal strength decreases as the base station to mobile station distance increases. This decrease in signal strength is named path loss. Path loss is a large-scale propagation model.

This section describes the radio propagation models implemented in this the simulations. These models are used to predict the received signal power at a point.

2.2.1.1. Free space model

The free space model is an idealized propagation model based on the following assumptions[10]:

1. There are no absorbing or reflective objects between the transmitter and the receiver.
2. The atmosphere behaves as a perfectly uniform and non-absorbing medium.
3. The earth is infinitely far away from the propagating signal.

The decrease in signal strength is inversely proportional to the square of the transmitter-receiver separation. The path loss is given by

$$\frac{P_r}{P_t} = G_t G_r \left(\frac{\lambda}{4\pi d} \right)^2 \tag{2.1}$$

where G_t is the transmitting antenna gain, G_r is the receiving antenna gain, λ is the wavelength of the propagating signal, and d is the distance between the transmitter and the receiver. The values of G_t and G_r range between 0 and 1. This is obviously a very deterministic model of propagation.

However, signal propagation takes place in the non-ideal atmosphere and near the ground for most realistic channels, which makes the free-space propagation model inadequate for predicting the path loss[10].

2.2.1.2. Two-ray ground reflection model

Since a single line-of-sight path between the base station and the mobile station, is rarely the only means of propagation in a mobile radio environment, using the free space propagation model alone is inaccurate for most channels. Alternatively, we can assume that the propagation takes place via a ground reflection path in addition to the direct path and this gives us the two ray ground model. This model, illustrated below in Figure 2.1, gives reasonably accurate predictions of path loss over distances of several kilometers for mobile systems with tall towers and for line-of-sight microcell channels in urban environments[11].

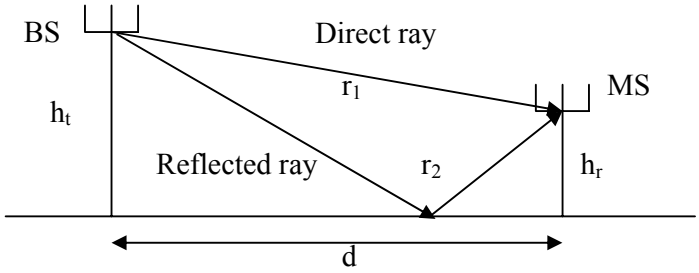

Figure 2.1: The direct ray and the reflected ray in the two-ray model[11]

The received power at distance d is predicted by[11]

$$\frac{P_r}{P_t} = G_t G_r \frac{(h_t h_r)^2}{d^4} \tag{2.2}$$

where G_t is the transmitting antenna gain, G_r is the receiving antenna gain, h_t is the height of the transmitting base station antenna in meters, h_r is the height of the receiving base station antenna in meters, and d is the distance between the transmitter and the receiver. This expression for path loss does not depend on the frequency. The values of G_t and G_r range between 0 and 1.

Compared to the free space propagation model, the loss predicted by this model increases as 40 dB/decade instead of 20 dB/decade. However, the two-ray model does not yield good results for short distances due to the oscillation caused by the constructive and destructive interference of the two rays. So, when d is small, the free space model is still used[12].

2.2.1.3. Hata model

A good prediction of path loss is not possible using analytical models and this has led to the development of empirical models based on measurements. Okumura made extensive power level measurements for different frequencies, antenna heights, and topographic conditions.

As a result of his field measurements, Okumura produced graphical path loss curves. Using these curves, Hata came up with an empirical formulation. This model is valid for the frequency range of 150 MHz to 1500 MHz. The standard formula for median path loss in urban areas is given by[13]

$$L_{50}(urban)(dB) = 69.55 + 26.16\log_{10} f_c - 13.82\log_{10} h_{te} - \alpha(h_{re}) + (44.9 - 6.55\log_{10} h_{te})\log_{10}(d) \quad (2.3)$$

where

f_c : frequency in MHz, from 150 MHz to 1500 MHz

h_{te} : effective transmitter antenna height, in meters, ranging from 30 m to 200 m

h_{re} : effective receiver antenna height, in meters, ranging from 1 m to 10 m

d : transmitter-receiver separation distance in km

$\alpha(h_{re})$: correction factor for effective mobile antenna height which is a function of the size of the coverage area.

There are correction equations for application to other environments. For a small to medium sized city, the mobile antenna correction factor is given by[13]

$$\alpha(h_{re}) = (1.1\log_{10} f_c - 0.7)h_{re} - (1.56\log_{10} f_c - 0.8)dB \quad (2.4)$$

and for a large city, it is given by[13]

$$\alpha(h_{re}) = 8.29(\log_{10} 1.54h_{re})^2 - 1.1dB \quad \text{for } f_c \le 300MHz \quad (2.5.a)$$

$$\alpha(h_{re}) = 3.2(\log_{10} 11.75h_{re})^2 - 4.97dB \quad \text{for } f_c \ge 300MHz \quad (2.5.b)$$

The path loss in a suburban area is given by[13]

$$L_{50}(dB) = L_{50}(urban) - 2[\log_{10}(f_c/28)]^2 - 5.4 \quad (2.6)$$

and for path loss in open rural areas[13]

$$L_{50}(dB) = L_{50}(urban) - 4.78(\log_{10} f_c)^2 - 18.33\log_{10} f_c - 40.94 \quad (2.7)$$

As long as the transmitter-receiver separation is greater than 1 km, the predictions of the Hata model are very close to the original Okumura model[13].

2.2.1.4. COST-231 extension to Hata model

The original Hata model was limited to 1500 MHz, but the PCS (Personal Communications Systems) systems were using frequencies on the order of 1900 MHz. This necessitated the European Co-operative for Scientific and Technical Research (EURO-COST) to form the COST-231 working committee to develop an extended version of the Hata model. COST-231 proposed the following formula to extend Hata's model to 2GHz[13].

$$L_{50}(urban)(dB) = 46.3 + 33.9\log_{10} f_c - 13.82\log_{10} h_{te} - \alpha(h_{re}) + (44.9 - 6.55\log_{10} h_{te})\log_{10}(d) + C_M \quad (2.8)$$

where $\alpha(h_{re})$ is defined in equations (2.4), (2.5.a), (2.5.b) and[13]

b

$$C_M = \begin{cases} 0\text{ dB} & \text{for medium sized city and suburban areas} \\ 3\text{ dB} & \text{for metro centers} \end{cases} \quad (2.9)$$

This extended model is restricted to the following range of parameters[13]:

f_c : 1500 MHz to 2000 MHz

h_{te} : 30 m to 200 m

h_{re} : 1 m to 10 m

d : 1 km to 20 km

2.2.2. Large-Scale and Small-Scale Fading

In addition to the distance-dependent attenuation of signal strength, the received signal strength undergoes random fluctuations due to the constructive and destructive combinations of multipath waves. Small-scale fading is the short-term fluctuation in the signal amplitude caused by the local multipath and is observed over distances of about half a wavelength. On the other hand, large-scale fading, a long-term variation in the mean signal level, is a result of movement over distances large enough to cause

significant variations in the path between the transmitter and the receiver. Large-scale fading is also known as shadowing and is a result of the mobile unit moving into the shadow of surrounding objects like buildings and hills[14].

2.2.2.1. Shadowing

Figure 2.2 below demonstrates the fading dips due to shadowing. According to measurements, the received power at two different locations with the same transmitter-receiver separation varies greatly. The overall path loss in this case may be modeled as a random variable lognormally distributed around the mean distance-dependent value[13].

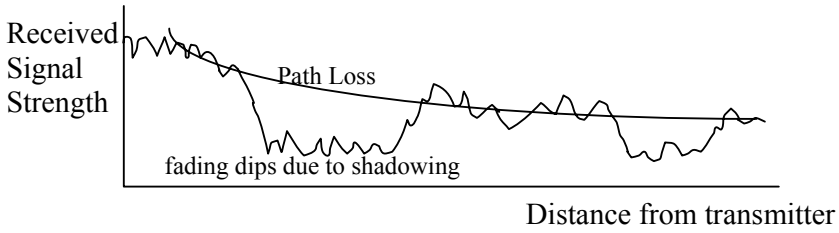

Figure 2.2: Shadowing[9]

The lognormal distribution models the random shadowing effects which occur over a large number of measurement locations with the same transmitter-receiver separation, but having different levels of obstructions on the propagation path[13].

A lognormal random variable has a Gaussian distribution if measured in decibels. Shadowing is a Gaussian random variable with zero mean and standard deviation calculated using measurements. The shadowing model extends the deterministic path loss models to a more realistic statistical model.

2.2.2.2. Multipath Rayleigh fading

Reflections off the obstructions between the base station and the mobile station create multiple propagation paths for the signal. These multipath signals may lead to signal cancellation, thus reducing the received signal power[9].

A simplified example is a signal arriving by two different paths to the mobile station as shown below in Figure 2.3.

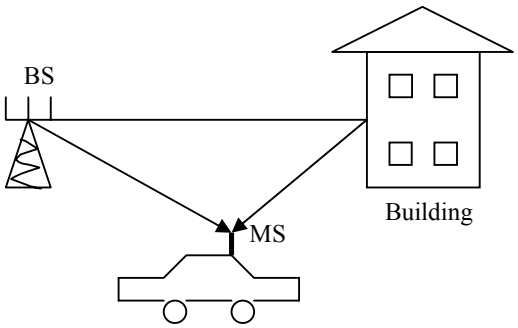

Figure 2.3: Signal arriving by two paths[9]

First, the direct signal from the base station is received. The second signal is reflected off a building and thus arrives at a later time. This causes phase difference between the reflected signal and the direct signal. Destructive interference occurs when the two signals are 180 degrees out of phase. In a real mobile environment, where there are many signals with phase differences, the received signal will be completely destructed at certain locations and times[9].

These drastic drops in signal strength, known as Rayleigh fading dips, follow a statistical distribution. For example, traveling at a constant speed of around 80 km/hr, a mobile subscriber will face many Rayleigh fading dips with a duration of a few milliseconds each[9]. Figure 2.4 below shows an example of Rayleigh fading dips generated using Simulink's Rayleigh Fading Block.

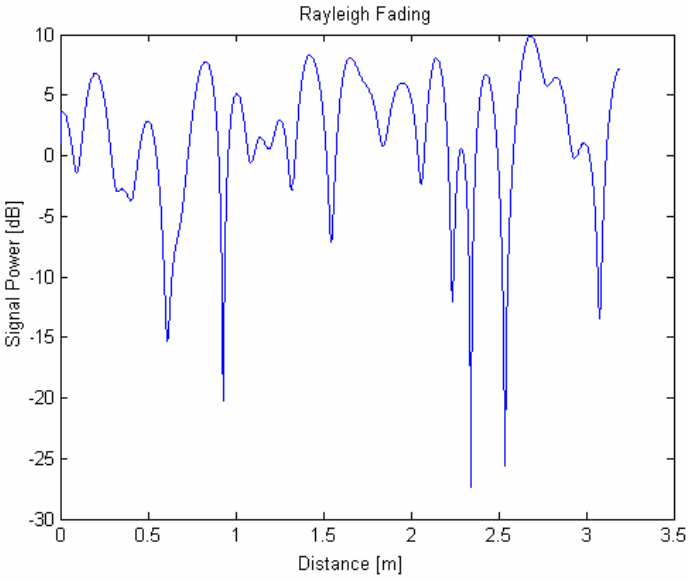

Figure 2.4: Rayleigh fading

In contrast to the fading dips due to lognormal shadowing, which are predictable, Rayleigh fading cannot be accurately predicted since it involves reflections from moving objects. The reflections from obstacles, such as other moving vehicles or mobile subscribers, in the proximity of the mobile subscriber is constantly changing, rendering them unpredictable[9].

There are two main factors that determine the number, duration, and location of Rayleigh dips experienced by the mobile subscriber[9]:

1. Frequency of the transmitted signal
2. Speed of the mobile subscriber

By changing frequency, the mobile subscriber could jump from a deep fade to a better signal level, since different frequencies have fading dips at different locations. Statistically, the distance between successive Rayleigh dips is about half a wavelength[9].

2.2.3. Overall Effect of Path Loss, Shadowing, and Fading

The total effect of path loss, shadowing, and Rayleigh fading resembles Figure 2.5 below[9]:

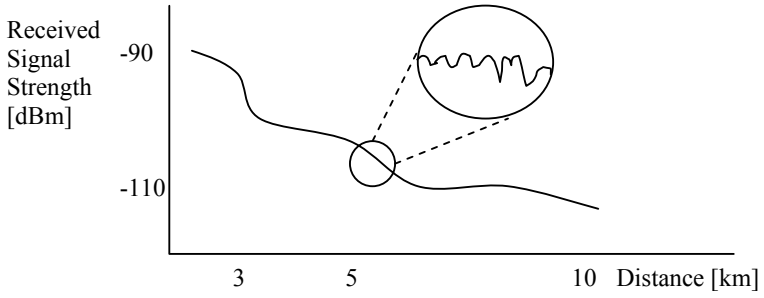

Figure 2.5: Received signal strength versus distance[9]

Taking the mean of these values removes the effects of Rayleigh fading and yields lognormal fading. Performing this averaging operation once more leaves us with what is known as the global mean[9].

Thus, around the global mean, the mobile subscriber experiences[9]:

- Fast variations in signal strength due to Rayleigh fading, typically lasting a few milliseconds
- Slow variations in signal strength due to shadowing, typically lasting a few seconds

2.3. Geolocation

In radiolocation systems, signals traveling between a mobile station (MS) and a group of fixed stations (FSs) are measured. Then, the length or direction (or both) of the propagation paths are determined using these measurements. Finally, the position of the mobile station is found using geometric techniques. Locating an MS in two dimensions generally requires measurements from three fixed stations. The prerequisite of a high accuracy radiolocation system is the existence of a line-of-sight path between the MS and the fixed stations. Otherwise, the estimates will be significantly erroneous[15].

The MS may formulate its own position by using signals received from the fixed stations. Then again, the position of the MS could be calculated at a central site using the measurements of received signal strength made at the fixed stations[15].

2.3.1. Location Techniques

The position of the MS can be estimated using angle-of-arrival (AOA), signal strength, or time-based techniques such as time-of-arrival (TOA) and time-difference-of arrival (TDOA). This section gives an overview of these techniques.

2.3.1.1. Angle of arrival

In the angle of arrival technique, first the arrival angles of a signal from a MS is measured at the fixed stations. Directive antennas or antenna arrays can be used to determine the AOA. The intersection of the lines-of-position, found through the use of simple geometry, yields the location[15].

2.3.1.2. Signal strength

Locating a mobile station using signal strength measurements requires a known path loss model. Since the signal strength is dependent on the distance between a MS and fixed stations, the MS lies on a circle centered at the fixed station and whose radius is mobile-fixed station separation. Therefore, in signal strength based radiolocation, the

mobile location is the intersection of these circles determined using at least three fixed stations[15].

Alternatively, premeasured signal strength contours around each fixed station can be used. Overlaying the contours of received signal strength measured at each fixed station maps these measurements to a location estimate. This technique would be more effective against shadowing[15].

2.3.1.3. Time-based techniques

Time-based location estimates the TOAs of a signal transmitted by the MS and received at three fixed stations or the TDOAs of a signal received at a minimum of two pairs of fixed stations. The mobile to fixed station separation is calculated by measuring the one-way propagation time between the MS and fixed station, in the TOA approach. In spread spectrum systems, the TOAs can be determined using correlation techniques[16]. Using an accurate timing reference at the mobile station yields measurements of the propagation time and since the signal travels at the speed of light, the distance between the fixed station and the mobile can be calculated. This distance defines a circle, centered at the fixed station, on which the MS must lie. At least three base stations are used to obtain a unique solution and the intersection of circles gives the position of the MS[15].

Since only the time difference is important in the TDOA approach, knowledge of the time of signal transmission is not required. The TDOA can be estimated by cross-correlating the signals received at a pair of BSs. The hyperbola is a curve of constant distance from two foci, thus the time-difference-of-arrival for two fixed stations defines a hyperbola, with the foci located at the two fixed stations[15].

The MS lies at the intersection of the hyperbolas. For three fixed stations receiving the signal from the MS, generally two non-redundant TDOA measurements can be made[15].

In the TOA approach, both the mobile station and the base stations need to have synchronous clocks, whereas in the TDOA approach such synchronization is not necessary.

2.3.2. Cellular System Geolocation

For a cellular geolocation system, the base stations serve the role of the fixed stations in the location techniques discussed. Cellular networks usually do not make use of the signal strength method because of the large variations in received signal strength resulting due to shadowing and multipath fading. AOA is an expensive technique, since it requires the placement of antenna arrays at the BSs. The AOA measurements can be obtained from array signal processing and do not depend on the type of cellular system deployed. The TOA and TDOA methods, in contrast to AOA, require that propagation times be obtained from MS signals. Each cellular system may use a different approach in obtaining this information[15].

Signal correlation methods are the simplest way of obtaining timing information for TOA or TDOA location. More specifically, finding the maximum values of the cross-correlations between the signals received at pairs of BSs will yield an estimate of the TDOAs for each pair of BSs[15].

For a WCDMA network, a way of locating the mobile station is to use pilot monitoring in the MS on the downlink. The MS monitors the pilot signal levels received from the BSs in order to assist in the handoff process. If the serving BS sends a pilot measurement request, the MS sends its response to all three BSs. Thus, TDOA estimates can be constructed from the code phases of each pilot relative to the pilot of the serving BS. The resolution of the code phase and the synchronization of the BSs determine the accuracy of the estimates[15]. The code phase resolution is limited to the chip time, T_c, and this implies a TDOA resolution of approximately 73 m (speed of light divided by the chip rate). The WCDMA standard does not require that the network be synchronized since some network operators are concerned about being dependent on a US-owned GPS system for synchronization. WCDMA aims to offer deep in-building coverage as well and in such an environment GPS would not be available.

Compared to the other systems, WCDMA can offer more accurate location estimates due to the high chip rate and good correlation properties of the spreading code sequences used[15].

2.3.3. Effect of Multipath on Location Error

In signal strength, AOA, TOA, and TDOA measurements, multipath propagation can introduce error. Multipath fading and shadowing cause variations in the signal strength that can be as great as 30-40 dB over distances in the order of half a wavelength. Signal strength averaging can help, but low mobility MSs may not be able to average out the effects of multipath fading and there will still be the variability due to shadowing. Using premeasured signal strength contours that are centered at the BSs can avoid errors due to shadowing, but this approach assumes a constant physical topography[15].

The TOA or TDOA estimates can be in error even when there is a LOS path between the MS and BS in time-based location systems. The presence of multipath fading affects the delay estimators using correlation techniques. Thus, the peak shifts away from the true value. The delay estimators will detect a delay in the vicinity of these later arriving signals[15].

2.4. Spread Spectrum

In spread-spectrum transmission, the original signal is spread to a larger bandwidth than the original signal would normally need. The original data is multiplied (XOR) with a spreading code that typically has a larger bandwidth (a higher frequency) than the original signal. Figure 2.6 below shows an example of this procedure. The spreading code bits are called chips and the bits in the data sequence are called symbols[7].

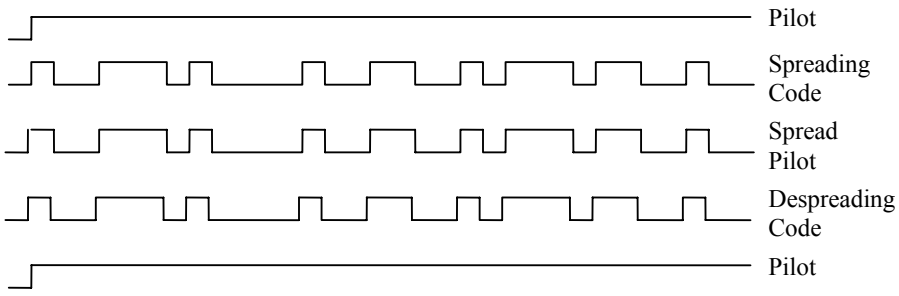

Figure 2.6: Spreading

The same code is used for spreading the signal on the transmitter end and despreading the wideband signal back to the original narrowband signal at the receiver end of the channel[7], as can be seen Figure 2.7 above.

At the cell level, the spreading codes are unique. This implies that a user can only despread the component of the received wideband signal that has been spread with the same code in the transmitter[7].

The low cross-correlation between different spreading codes allows several wideband signals to coexist on the same frequency without severe mutual interference. A wideband signal is just like background noise compared with the original signal since its energy is spread over a very large bandwidth. In other words, its power spectral density is small. When the wideband signal consisting of the combination of several signals spread with different spreading codes is correlated with the particular spreading code, only the original signal with the corresponding spreading sequence is despread, while all the other component signals remain spread. As long as the power of the despread signal is a few decibels higher than the interfering noise power, the original signal can be recovered in the receiver[7].

A wideband carrier does not actually increase the capacity of the allocated bandwidth. Theoretically, a set of narrowband carriers occupying the same bandwidth would be able to convey as much data as the wideband signal. However, it is possible to reuse the same frequency in adjacent cells, since the signals in a wideband system are more resistant to intercell interference. This means that the frequency reuse factor is one, while in typical GSM systems the value is at least four; that is the same frequency can be used at every fourth cell at most. This provides a substantial capacity gain over narrowband systems[7].

In WCDMA, base stations use a long scrambling code to reduce the interference from the channels in the adjacent cells. The primary scrambling code of each base station is used to separate various base stations[7]. The long scrambling codes are from the Gold codes constructed by using two pseudonoise (PN) sequences. The long code used on the forward pilot channel is 38400 chips of a $2^{18} - 1$ Gold code.

The power spectral density of a random data stream before transmission coding is essentially limited to $1/T$ Hz for a non-return-to-zero (NRZ) unipolar format. This means, for example, that a 100 Mbit/s NRZ signal could be transmitted without serious

degradation down a channel of 100 MHz bandwidth. However, this format is not suited to most transmission lines[6].

The power spectral density is zero at the bit frequency, so it is impossible to phase lock a receiver clock directly to the signal. For random data, a polar NRZ code (for example, 1=+1V, 0=-1V) will remove the DC component, but the power spectral density will still be significant near 0 Hz. However, most communication channels have a bandpass characteristic. Therefore, the signal needs to be spread before transmission[6].

2.4.1. Scrambling Code Construction as Specified by 3GPP

This section describes the creation of the scrambling code exactly as it is specified by 3GPP[17].

The scrambling code sequences are constructed by combining two real sequences into a complex sequence. Each of the two real sequences are constructed as the position-wise modulo-2 sum of 38400 chip segments of two binary m-sequences generated by means of two generator polynomials of degree 18. The resulting sequences thus constitute segments of a set of Gold sequences. The scrambling codes are repeated for every 10 ms radio frame. Let x and y be the two sequences respectively. The x sequence is constructed using the primitive (over Galois field 2) polynomial $1 + X^7 + X^{18}$. The y sequence is generated using the polynomial $1 + X^5 + X^7 + X^{10} + X^{18}$.

The sequence depending on the chosen scrambling code number n is denoted z_n, in the sequel. Furthermore, let $x(i)$, $y(i)$, and $z_n(i)$ denote the i^{th} symbol of the sequence x, y, and z_n, respectively[17].

The m-sequences x and y are constructed as:

Initial conditions:

$$x(0) = 1, x(1) = x(2) = \ldots = x(16) = x(17) = 0 \quad (2.1)$$

$$y(0) = y(1) = \ldots = y(16) = y(17) = 1 \quad (2.2)$$

Recursive definition of subsequent symbols:

$$x(i+18) = x(i+7) + x(i) \ modulo\ 2,\ i = 0, \ldots\ 2^{18} - 20 \quad (2.3)$$

$$y(i+18) = y(i+10) + y(i+7) + y(i+5) + y(i) \ modulo\ 2,\ i = 0, \ldots\ 2^{18} - 20 \quad (2.4)$$

Figure 2.7 below illustrates the shift register implementation.

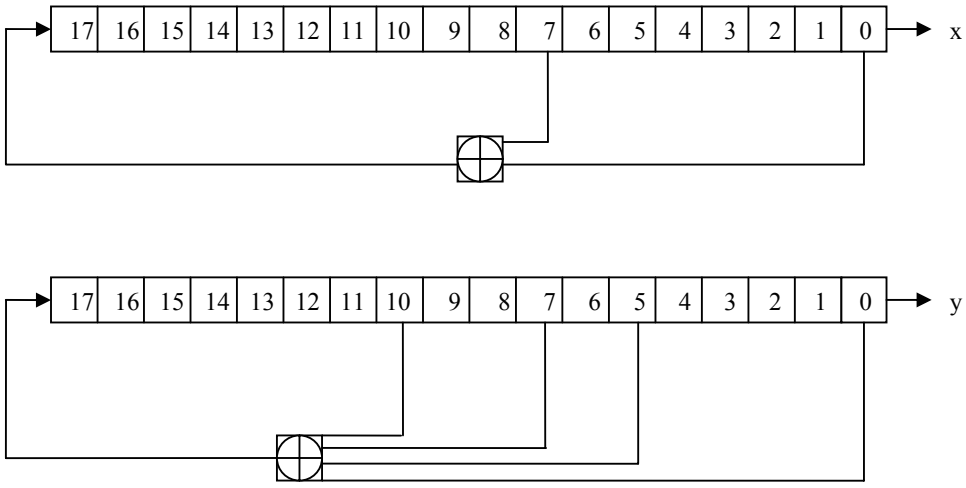

Figure 2.7: Shift register implementation of the m-sequences x and y

The n^{th} Gold code sequence z_n is then defined as[17]

$$z_n(i) = x((i+n) \text{ modulo } (2^{18}-1)) + y(i) \text{ modulo } 2,\ i = 0, \ldots\ 2^{18}-2. \qquad (2.5)$$

These binary sequences are converted to real valued sequences Z_n by the following transformation: for $i = 0, \ldots\ 2^{18}-2$, if $z_n(i)=0$, then $Z_n(i)=1$, and if $z_n(i)=1$, then $Z_n(i) = -1$.

Finally, the n^{th} complex scrambling code sequence $S_{dl,n}$ is defined as[17]:

$$S_{dl,n}(i) = Z_n(i) + j\, Z_n(i+131072),\ i = 0, 1, \ldots 38399. \qquad (2.6)$$

The pattern from phase 0 up to the phase of 38399 is repeated[17].

CHAPTER 3

SIMULATION TECHNIQUES

This chapter describes the simulations conducted to evaluate the performance of a WCDMA geolocation system. The simulations can be divided into the following three parts:

1. Propagation model analysis
2. Downlink simulator
3. Geolocation system

The cellular system simulated in this project has a 19-cell 3-tier 3-sector hexagonal cell topology with three directional antennas at the base station. The directional antenna of each sector has a 120-degree beamwidth. For the sake of simplicity, the cells are represented as hexagonal areas. The signal-to-interference ratio for the beta sector, shown in Figure 3.1 below, of the center cell was calculated using first the free space model, then the two-ray model, and finally the Hata model. The signal from the base station of the center cell was considered to be the desired signal and the signals from the 3-sectors of the remaining 18 cells the interference. Due to the symmetric nature of the cell topology, the signal-to-interference values in one cell will be representative of the values at the other neighboring cells.

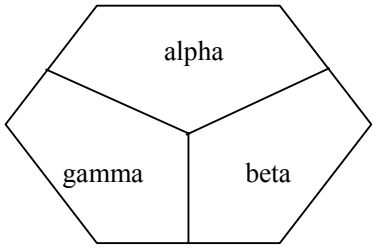

Figure 3.1: The three sectors of a 3-sector hexagonal cell

In such a system, the channel is characterized by distance loss, shadow loss, and multipath fading. The shadow loss is lognormally distributed. In this simulation, it is assumed to be a normal random variable with mean 0 and standard deviation 8 dB. This is the position dependent lognormal fading exponent. This standard deviation can be easily changed.

A toolbox was developed in Matlab Simulink to simulate path loss, fading, and the shadowing effects. The path loss models implemented are the free space model, two-ray ground reflection model, the extended Hata model, and shadowing. Rayleigh fading was used for the fading model and the TDOA method was used for the geolocation system.

3.1. Propagation Model Analysis

The function drawtier.m draws a central three-sector hexagonal cell centered on the coordinates (x_{coor}, y_{coor}) and the 6 hexagonal cells surrounding it, using the function drawcell.m. In return, drawcell.m draws a hexagonal cell of unit side length centered on the coordinates (x_p, y_p). Figure 3.2 below illustrates the system topology. This plot is obtained using the functions mentioned above. The hexagons are of unit length in this case. They can be scaled by any length desired. In the simulations, each hexagonal cell has a side length of 5 km.

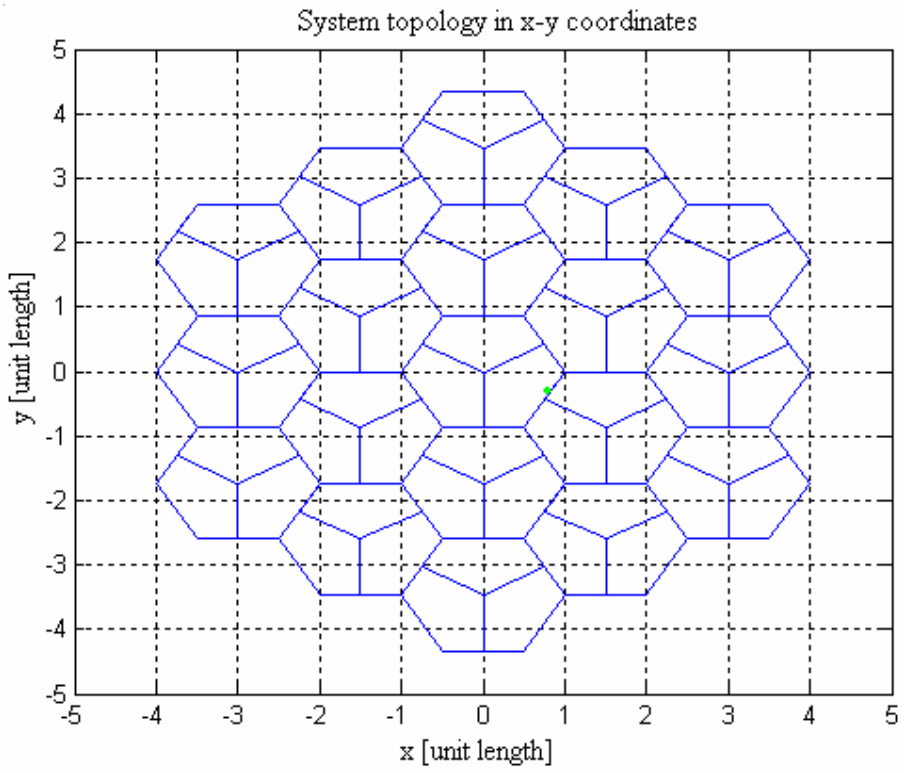

Figure 3.2: The 19-cell system and a random MS plotted by plotpoint.m

3.1.1. Effect of Antenna Directivity

First, the three directional antennas used for the three sectors were analyzed using antennagain.m. The antenna patterns are described by the equations below.

$$G_{alpha} = \left\| \cos^{n}(\theta/2 - \pi/4) \right\| \tag{3.1}$$

$$G_{beta} = \left\| \cos^{n}(\theta/2 - 2\pi/3 - \pi/4) \right\| \tag{3.2}$$

$$G_{gamma} = \left\| \cos^{n}(\theta/2 + 2\pi/3 - \pi/4) \right\| \tag{3.3}$$

The exponent n is set to 5. Below in Figure 3.3 is the polar plot of the three directional antenna patterns obtained using antennagain.m.

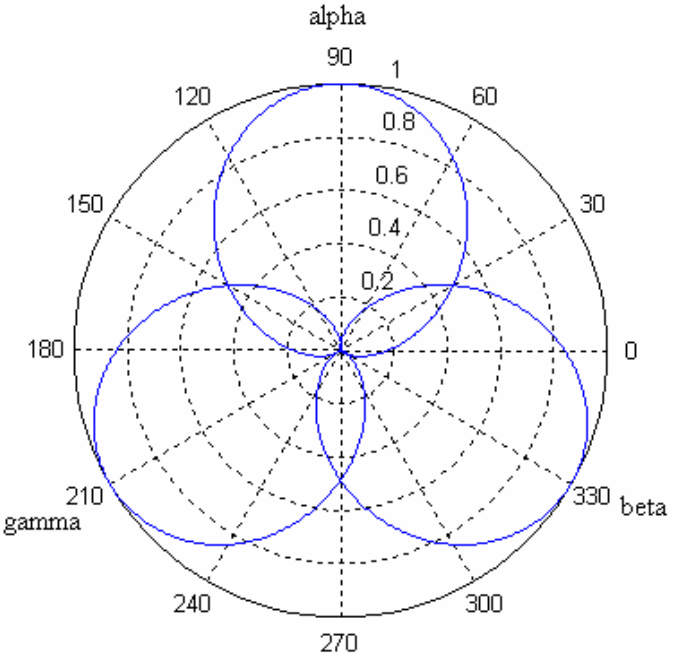

Figure 3.3: Polar plot of the three directional antenna gains

Figures 3.4, 3.5, and 3.6 below show the variation of antenna gain expressed in dB versus the angle between the transmitter and the receiver.

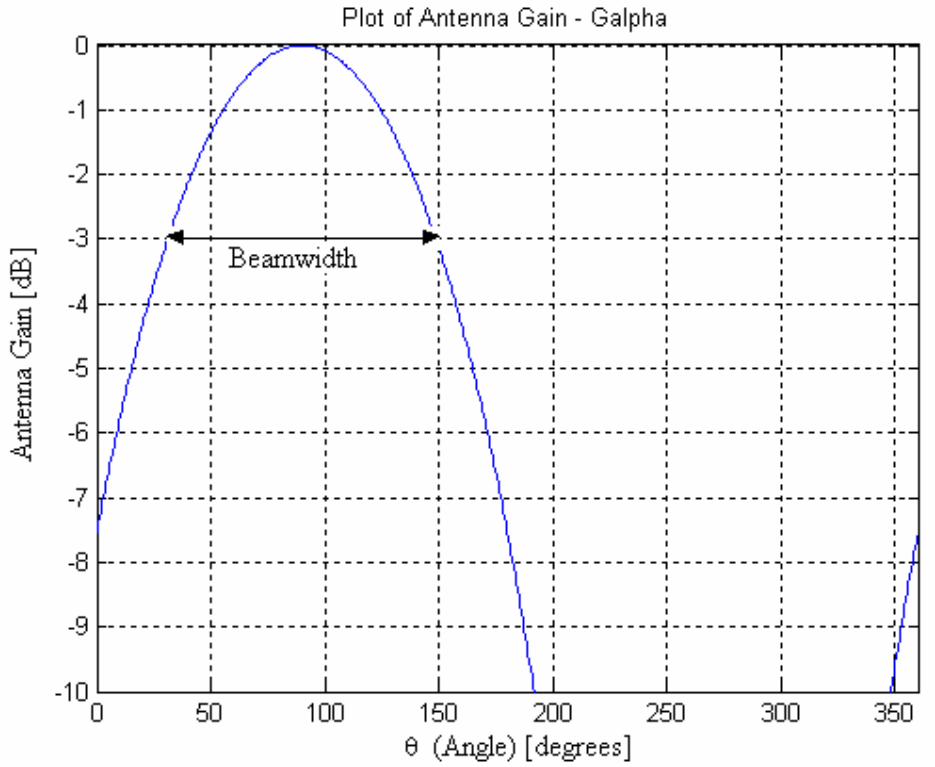

Figure 3.4: Antenna gain of the alpha sector antenna in dB versus the angle

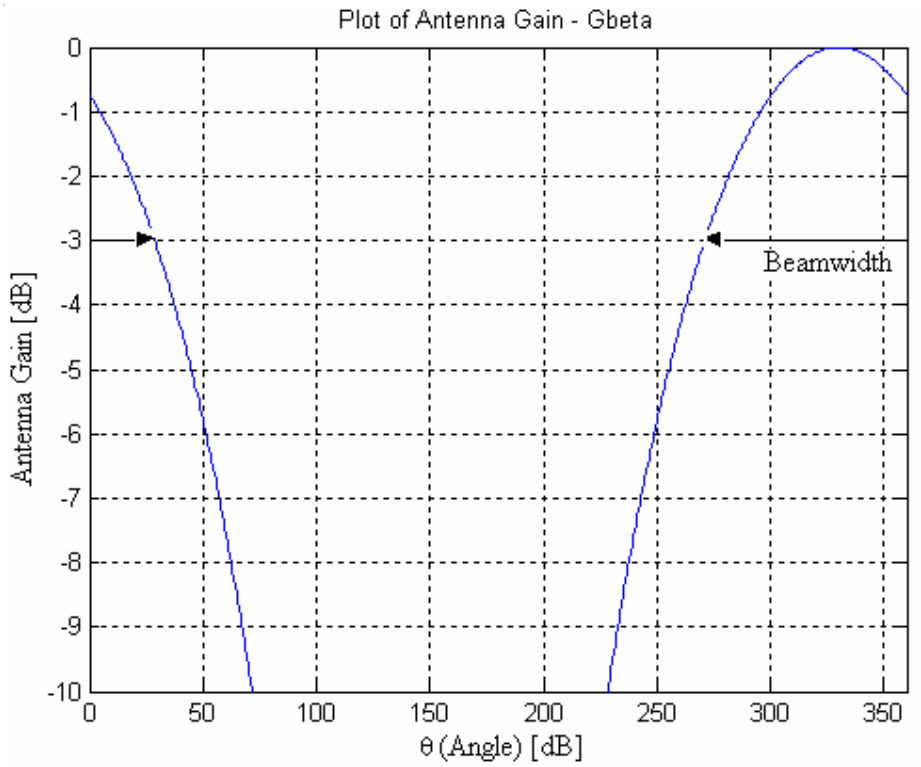

Figure 3.5: Antenna gain of the beta sector antenna in dB versus the angle

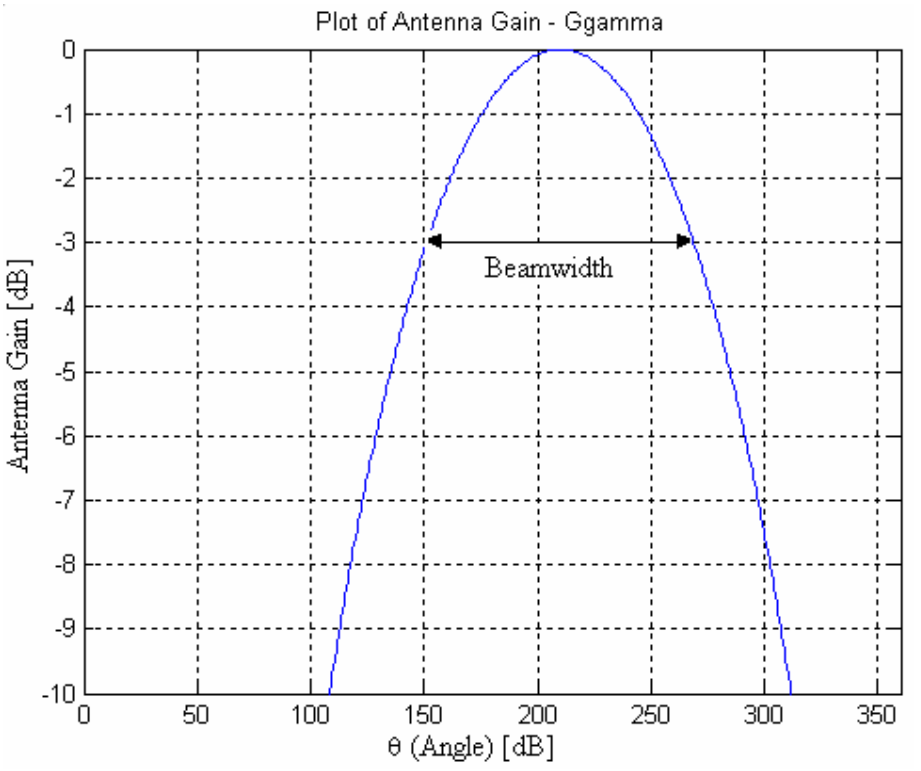

Figure 3.6: Antenna gain of the gamma sector antenna in dB versus the angle

The three figures above show that the antenna beamwidth for all three sectors is 120 degrees. The antenna beamwidth is the difference between the two angles where the antenna gain drops to -3 dB.

The function degree.m finds the angle (in degrees) between the transmitter and the receiver and this angle is used to calculate the antenna gain in that direction. Figure 3.7 below demonstrates which angle is defined as the angle between the transmitter and the receiver.

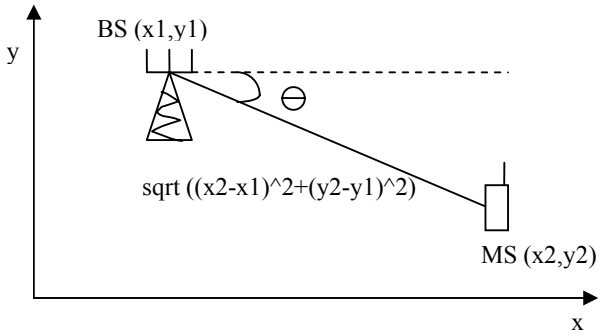

Figure 3.7: The degree between the BS and the MS as calculated by degree.m

In addition, the function dest.m finds the distance between two points whose coordinates are described by (x_1, y_1) and (x_2, y_2). This distance is shown above in Figure 3.7 along with the angle between the two locations.

The function gain.m, given the angle and the sector number, finds the gain of the chosen directional antenna in that direction. This gain ranges between 0 and 1.

3.1.2. Path Loss Models

Next, the free space, two-ray, and extended Hata path loss models were analyzed in Matlab.

The function contourfreesp.m calculates the signal from center cell located at (0,0). Sector 2 of this center cell is assumed to be the transmitter. Interference is first set equal to the signal from sector 1, then the signal from sector 3 is added to it. Then, we loop through all three sectors of the interfering 18 cells and find the signal-to-interference ratio by dividing the signal by the interference.

The functions contourtworay.m and contourCOST231.m are similar in structure to contourfreesp.m,, but the path loss models used in evaluating the signal and the interference are the two-ray model and the COST-231 model respectively, instead of the free space model.

3.1.2.1. Free space model

The antenna patterns described above in Section 3.1.1 are used in evaluating free space path loss. The values of G_t and G_r range between 0 and 1 depending on the reference angle. The wavelength, λ, was taken to be $(3\times10^8\, m/s)/(2\times10^9\, Hz) = 0.15$m.

The function freespace.m takes G_t, G_r, and the distance, d, as its inputs and returns the ratio of the received power P_r to the transmitted power, P_t, at that distance. Figure 3.8 below shows a contour plot of this path loss obtained using contourfreesp.m. The dashed line indicates the borders of the beta sector. The direction of maximum antenna gain for this sector is shown by a line passing through 330°.

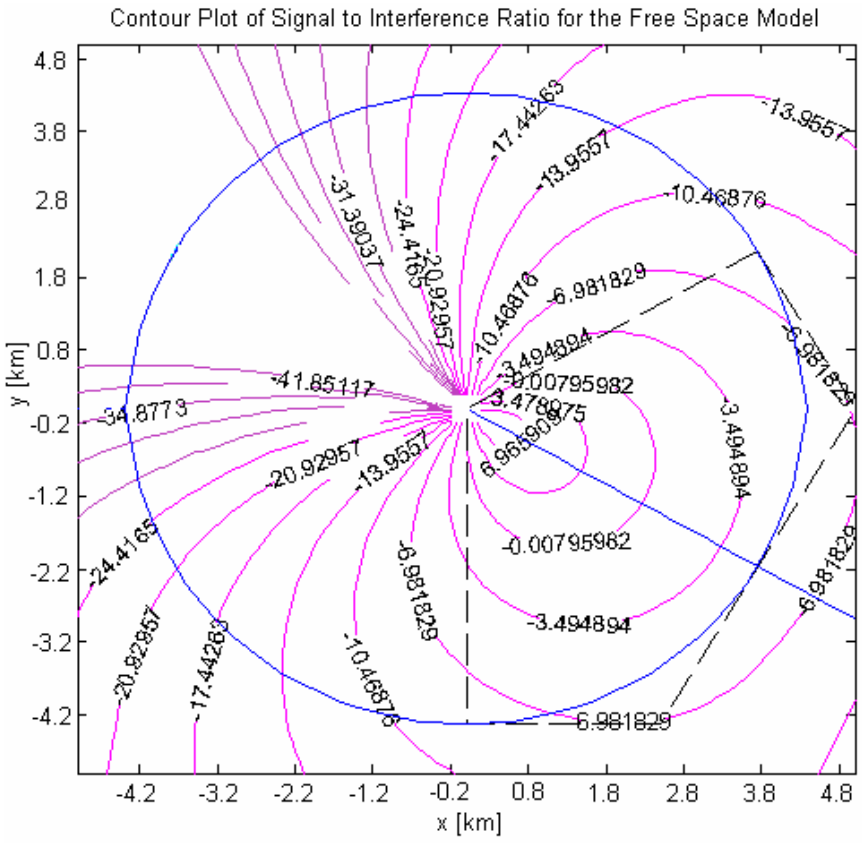

Figure 3.8: Contour plot of the signal to interference ratio for the free space model

3.1.2.2. Two-ray model

This model again makes use of the antenna patterns. The transmitter height was set to 50m and the receiver height is set to 1.5m. The values of G_t and G_r range between 0 and 1 depending on the reference angle. The wavelength, λ, was taken to be $(3\times10^8 m/s)/(2\times10^9 Hz) = 0.15m$.

The function tworay.m takes G_t, G_r, and the distance, *d*, as its inputs and returns the ratio of the received power P_r to the transmitted power, P_t, at that distance. Figure 3.9 below shows a contour plot of this path loss obtained using contourtworay.m. The dashed line indicates the borders of the beta sector. The direction of maximum antenna gain for this sector is shown by a line passing through 330°.

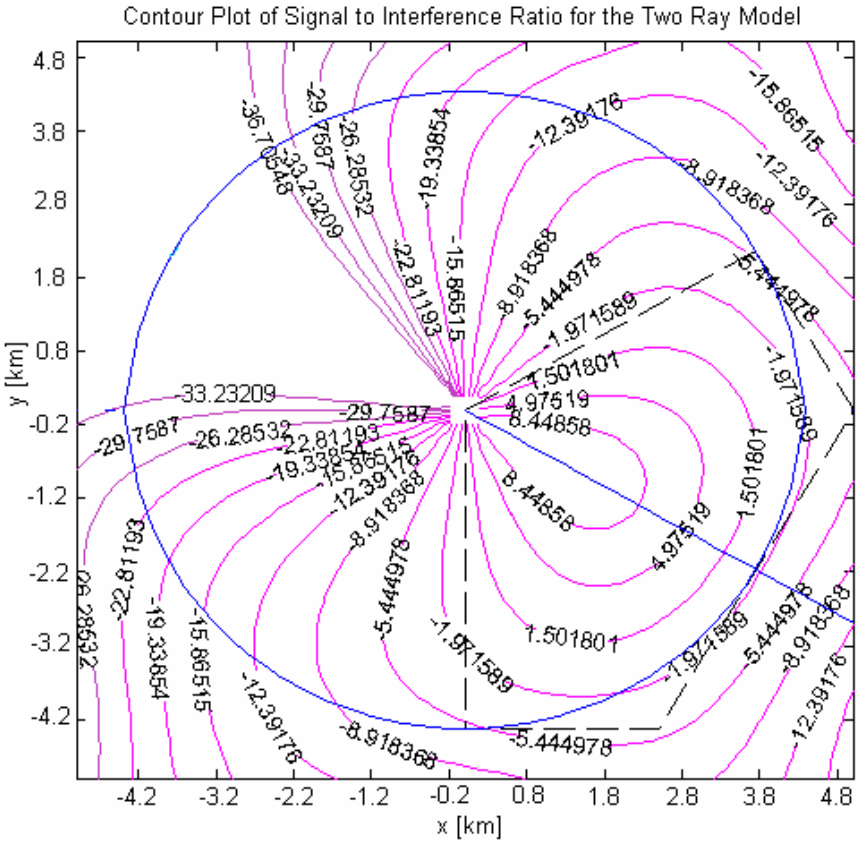

Figure 3.9: Contour plot of signal to interference ratio for the two-ray model

3.1.2.3. COST-231 extension to Hata model

This model again makes use of the antenna patterns. The transmitter height was set to 50m and the receiver height is set to 1.5m. The values of G_t and G_r range between 0 and 1 depending on the reference angle. The wavelength, λ, was taken to be $(3\times10^8\, m/s)/(2\times10^9\, Hz) = 0.15m$.

The function cost231.m takes G_t, G_r, and the distance, d, as its inputs and returns the ratio of the received power P_r to the transmitted power, P_t, at that distance. Figure 3.10 below shows a contour plot of this path loss obtained using contourCOST231.m. The dashed line indicates the borders of the beta sector. The direction of maximum antenna gain for this sector is shown by a line passing through 330°.

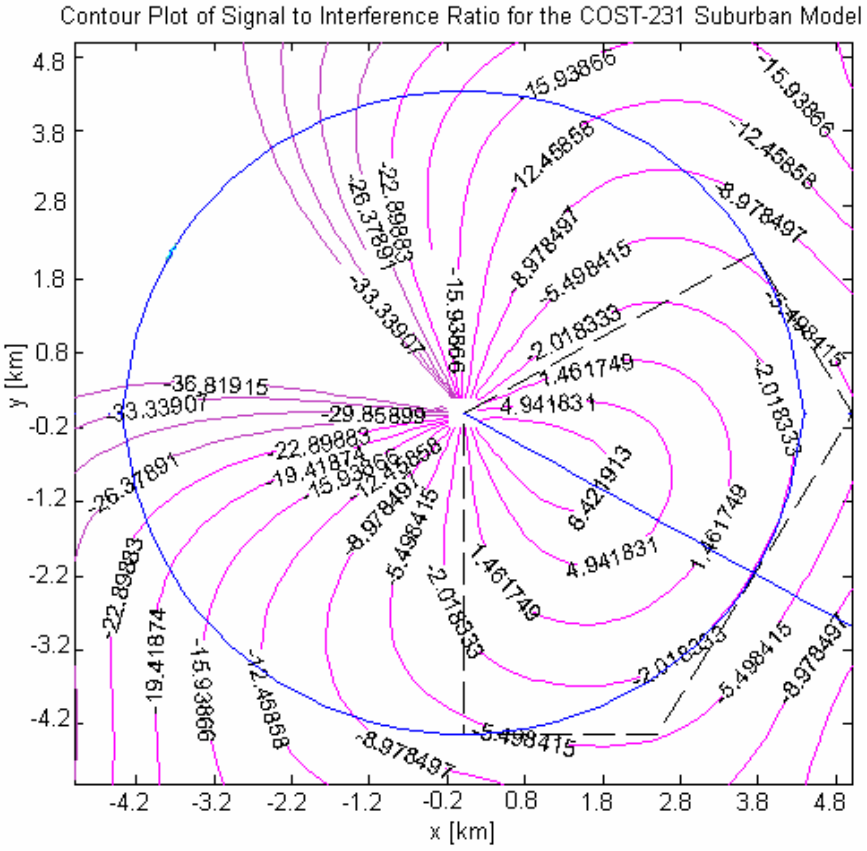

Figure 3.10: Contour plot of the signal to interference ratio for the COST-231 model

3.1.3. Signal Levels at Random Locations

In addition to the contour plots above in Section 3.1.2, we can observe the signal, interference, and the signal-to-interference ratio at random locations within the beta sector. Figure 3.11 below, generated by coversector.m, shows 2000 random MS locations covering the whole beta sector.

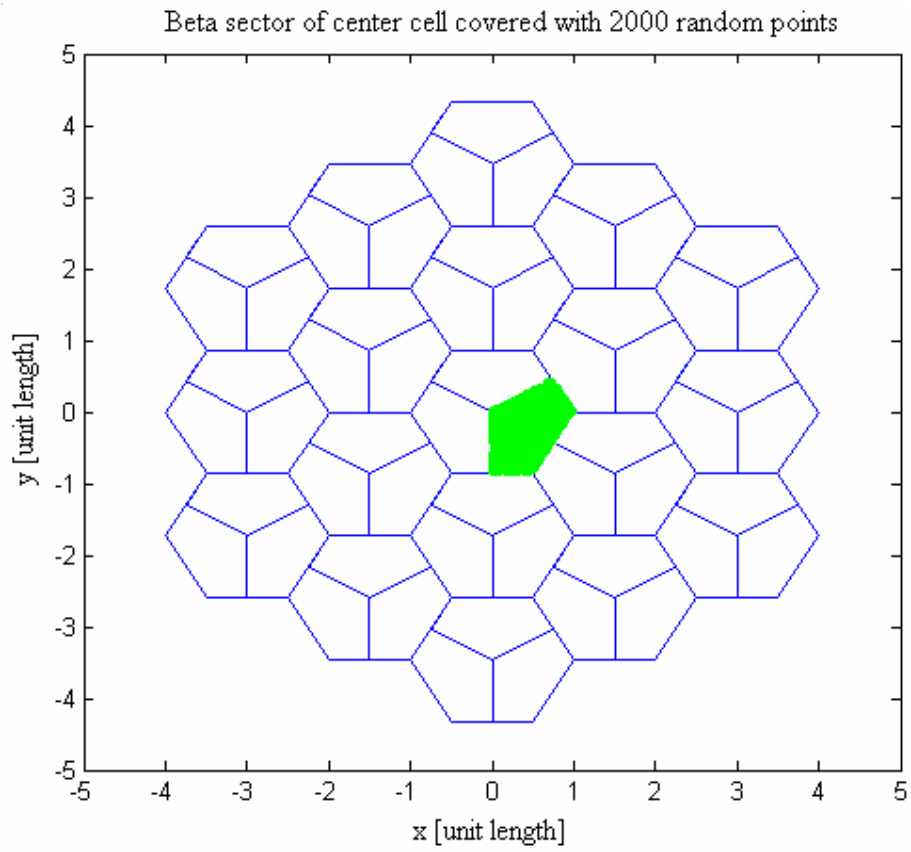

Figure 3.11: Beta sector covered by 2000 random points

3.1.4. Lognormal Shadowing

The function complosslogn.m demonstrates an example of a lognormally distributed path loss. Shown below in Figure 3.12 is the plot of lognormal shadowing for 8 dB standard deviation. The shadowing random variable is generated for every

1.5m, corresponding to 10 wavelengths of a 2 GHz signal. The path loss model is free space.

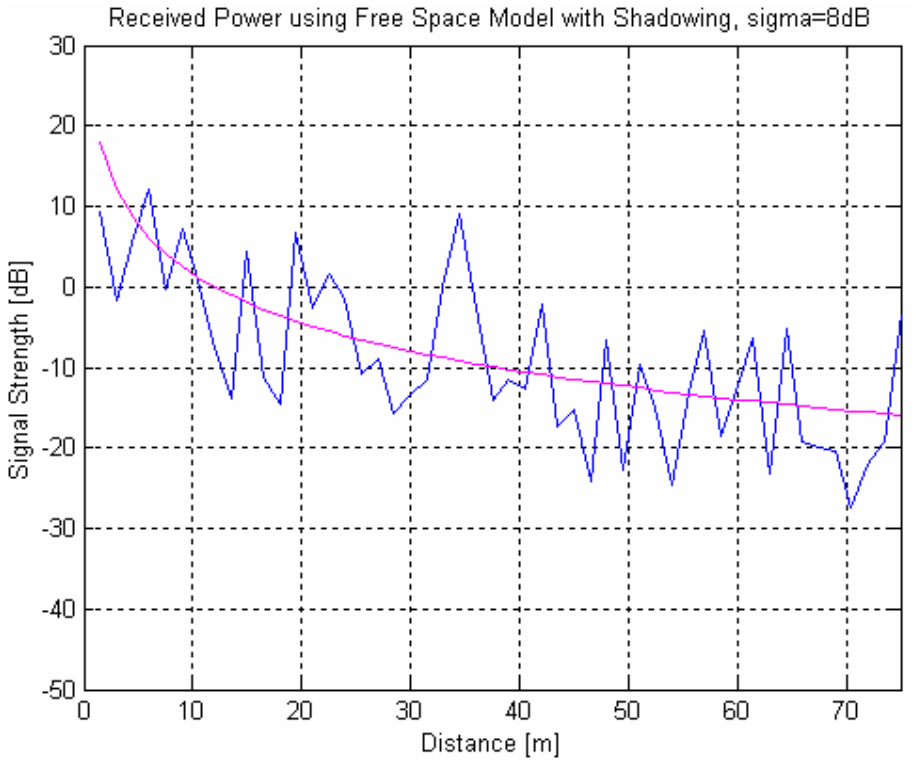

Figure 3.12: Received power vs. distance for the free space model with and without shadowing

3.2. Downlink Model

This section discusses the end-to-end (transmitter-to-receiver) simulation model that was developed for the forward link of the WCDMA system.

Blocks from the Communications Blockset, DSP Blockset, and the CDMA demo[19] were used extensively. Figure 3.13 below illustrates the WCDMA forward channel. The transmitter section includes spreading and filtering. The receiver section includes filtering, despreading, and correlation. Rayleigh fading and additive white Gaussian noise blocks model the effects of the channel between the transmitter and the receiver.

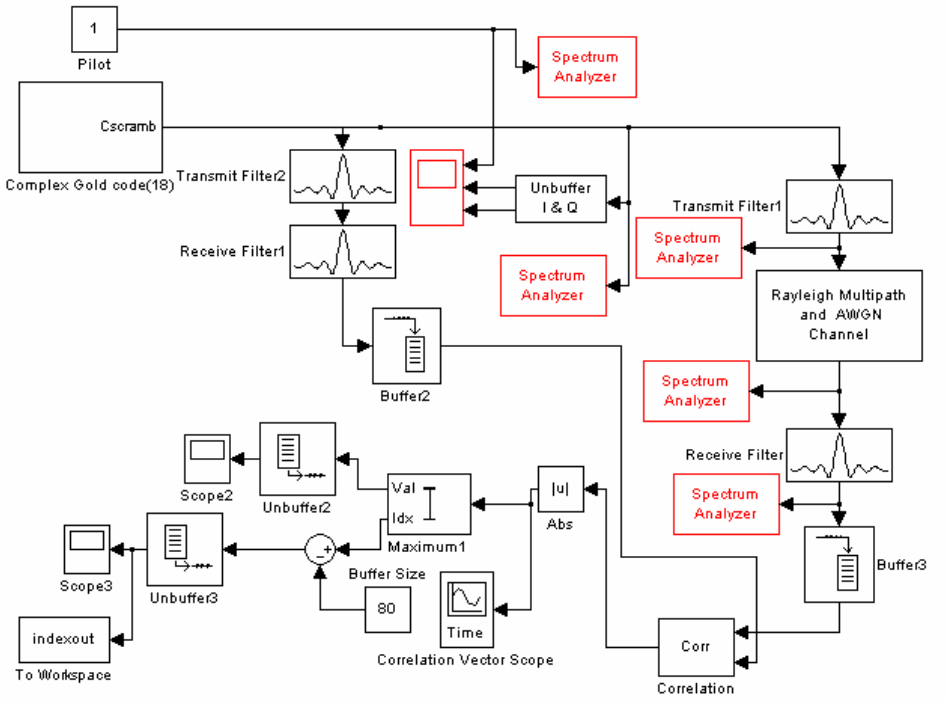

Figure 3.13: The model end2end.mdl

The pilot channel is a constant symbol. The channel coding operations in the WCDMA system use 10 ms frames for all channels.

The WCDMA system requires spreading of the spectrum using a PN sequence. In WCDMA, the rate of this PN sequence is 3.84 Mchips/s. This causes the resulting bandwidth of the spread signals to be about 4.6848 MHz.

The WCDMA system uses a complex Gold code. This Gold code is a pair periodic binary PN sequences with a period of 2^{18}-1. These sequences are used for spreading and despreading signals into in-phase and quadrature components. Multiple base stations use different masks in the PN sequence generator to obtain different Gold codes.

The role of the transmitter section is to generate the spread signal that contains the pilot channel. The transmitter components are the pilot signal, the spreading and the transmit filter.

The Gold code generator block generates the complex spreading code. The pilot signal is spread with the in-phase and quadrature components of the PN sequence. The signal generated is processed by pulse shaping transmit filter block, which generates the modulated I and Q waveforms.

The receiver section of the system is responsible for the detection of the time delay. The operations performed in this section include the receive filtering and the correlator.

3.2.1. Base Station Spreading

The Pilot channel of the forward WCDMA link is spread in quadrature by a pair of Gold sequences with a fixed spreading rate. The spread signal is filtered at baseband prior to transmission. Direct sequence spreading can be seen as a form of BPSK modulation, just multiplying a signal by +1 or -1.

3.2.1.1. Generation of the complex code

The generation of the complex spreading code is outlined below:

1. We execute goldutra3write384.mdl to generate the 18-stage PN sequence and convert it from unipolar to bipolar format (0/1 $\rightarrow$ +1/-1). We now have znprime whose length is 38400+131072=169472 chips. We send znprime to workspace using the variable name yout. Figure 3.14 below illustrates this model.

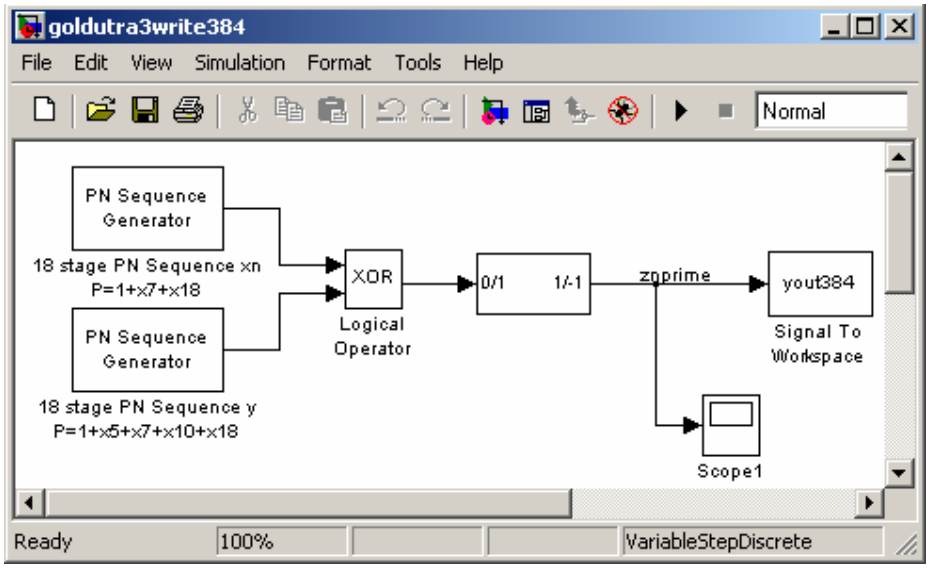

Figure 3.14: The model goldutra3write384.mdl

2. We run the code in aftergwrite384.m. This shifts yout by 131072 bits and stores this shifted version in the variable youtshift384 (size 38400). The original yout is truncated to 38400 bits and stored in the variable youtnoshift384. The time variable tout is truncated to 38400 chips.
3. We execute goldutraread3_384.mdl to save the variable youtshift384 in the matrix file shift384.mat. This is illustrated below in Figure 3.15.

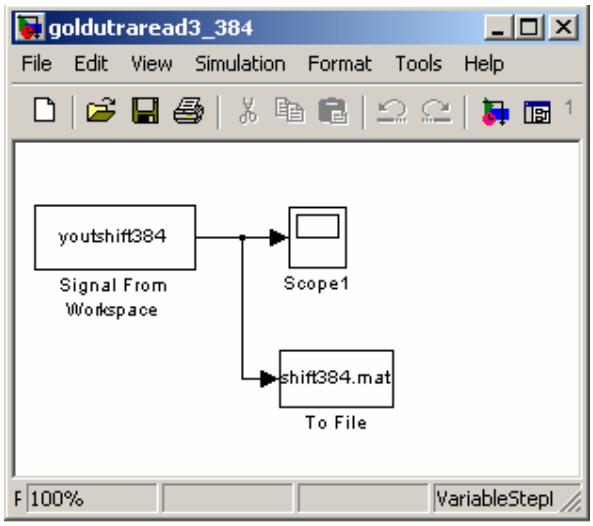

Figure 3.15: The model goldutraread3_384.mdl

4. We execute goldutrareadnoshift384.mdl, which is similar to the model goldutraread3_384.mdl in Figure 3.15 above, except youtshift384 is replaced by youtnoshift384, and shift384.mat is replaced by noshift384.mat. Thus, we save the variable youtnoshift384 in the matrix file noshift384.mat.

3.2.1.2. Transmit filter

The signal generated is processed by the pulse shaping transmit filter block, which generates the modulated I and Q waveforms. The transmit filter consists of upsampling by a factor of 8 and filtering using a square-root raised cosine filter. 3GPP[20] specifies a square-root raised cosine filter (with a roll-off factor of 0.22) to minimize the intersymbol interference, which results in a bandwidth of

$$\Delta f = CR(1+\alpha) = 3.84(1+0.22) = 4.6848 \text{ MHz}$$

where Δf is the channel separation, CR is the chip rate, and α is the roll-off factor.

The transmit filter serves the purpose of spectral containment and this subsystem is shown below in Figure 3.16.

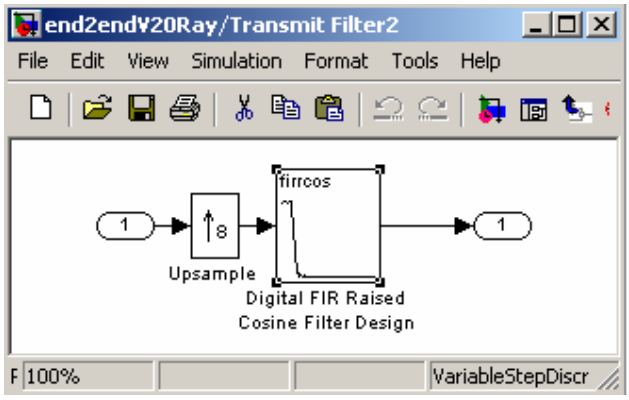

Figure 3.16: The transmit filter block

Figure 3.17 below shows the parameters for the square-root raised cosine filter.

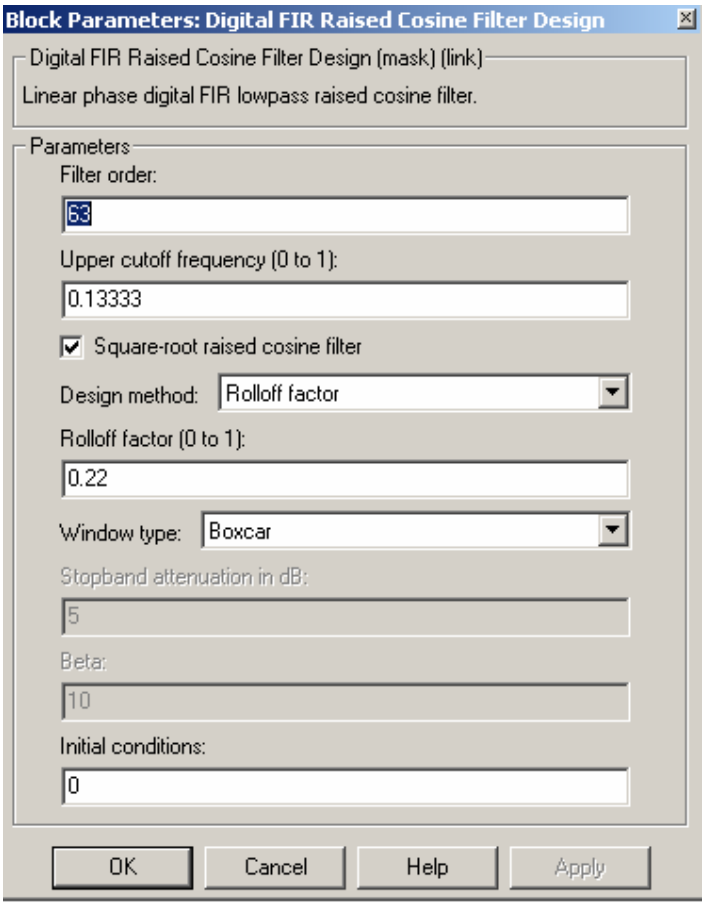

Figure 3.17: The transmit filter parameters

3.2.1.3. Rayleigh fading and AWGN channel

The Rayleigh Multipath and AWGN Channel Subsystem simulates the effects of the multipath propagation of a Rayleigh fading channel. The complex white Gaussian noise represents the cochannel interference. This subsystem is given below in Figure 3.18.

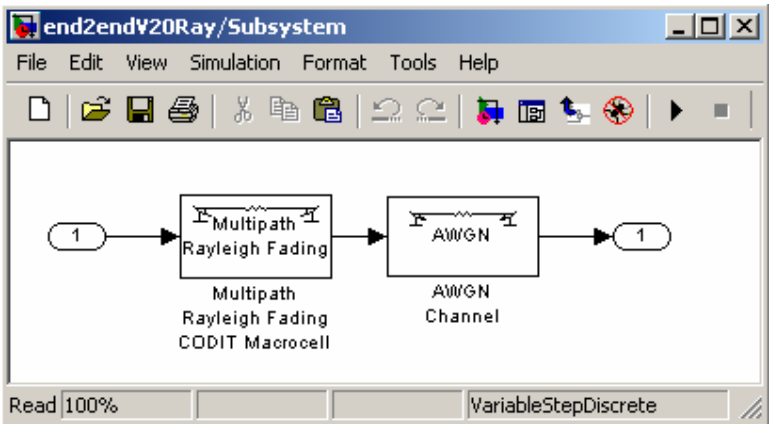

Figure 3.18: Rayleigh fading and AWGN block

The parameters for the Rayleigh fading channel are given below in Figure 3.19. The Doppler frequency is chosen as 175.92 Hz, corresponding to a mobile speed of 95 km/h. The delay vector and the gain vector, in this case, are the values specified by the CODIT model. Rayleigh fading is a worst-case scenario where no direct line of sight path exists and is most perceptible in urban areas.

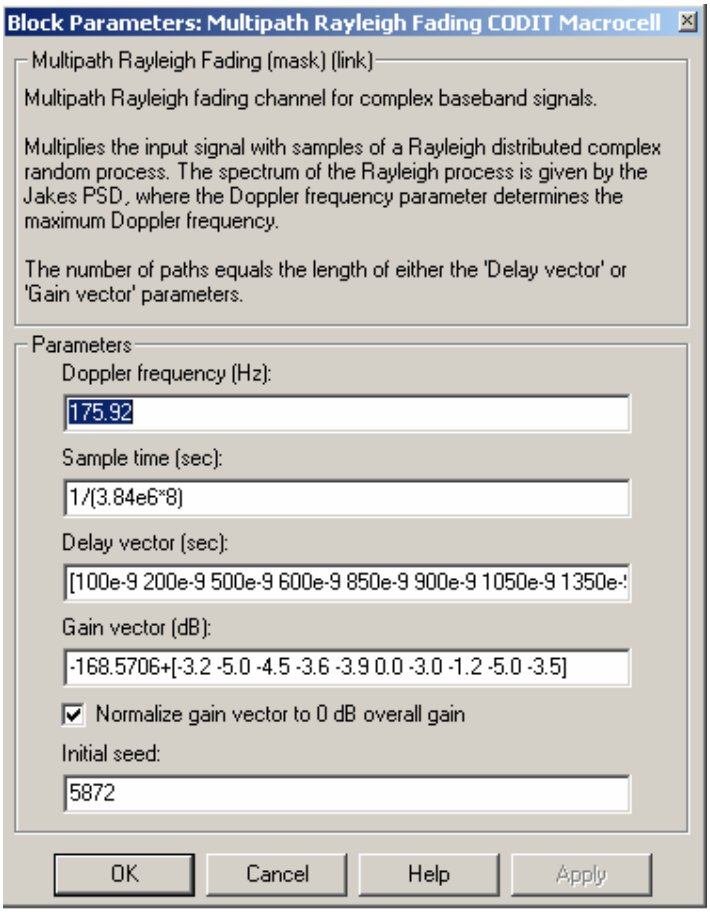

Figure 3.19: Rayleigh fading block parameters

The parameters for the AWGN channel are given below in Figure 3.20. The detection performance of the correlator improves with an increase in the signal-to-noise ratio specified in the AWGN Channel block.

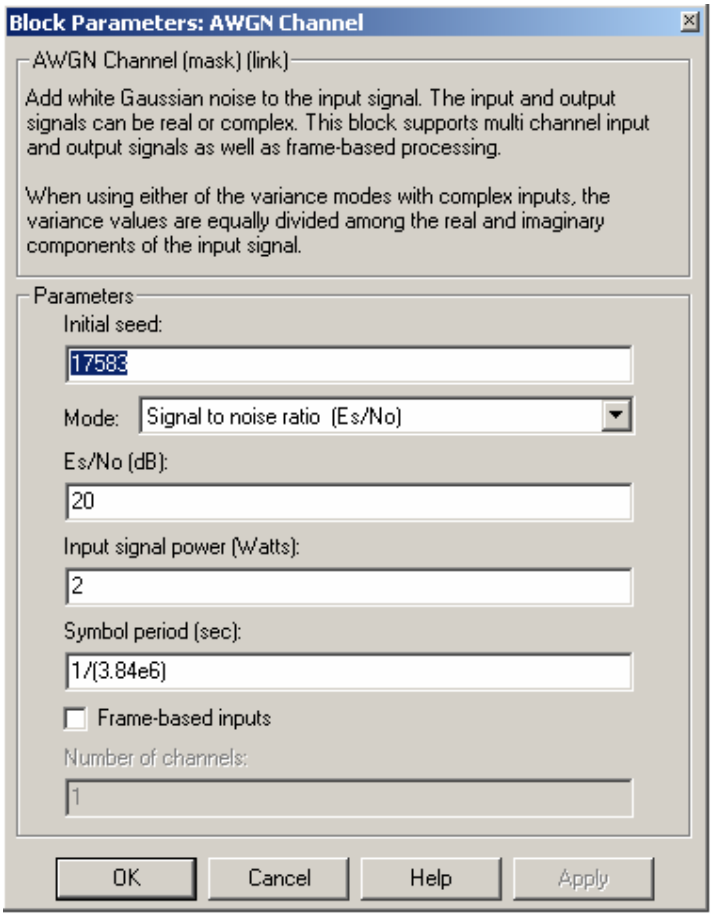

Figure 3.20: AWGN channel parameters

The multipath delay profile models used are ATDMA Macro, CODIT Macro, ITU Vehicular A, and ITU Vehicular B. These models are given below in Tables 3.1 through 3.4.

Table 3.1: Multipath delay profile for the ATDMA Macro model[21]

Delay [ns]	Relative Gain [dB]
0	0
380	-10
930	-22.7
1940	-24.7
2290	-20.7
2910	-22.1

Table 3.2: Multipath delay profile for the CODIT Macro model[21]

Delay [ns]	Relative Gain [dB]
100	-3.2
200	-5.0
500	-4.5
600	-3.6
850	-3.9
900	0.0
1050	-3.0
1350	-1.2
1450	-5.0
1500	-3.5

Table 3.3: Multipath delay profile for ITU Vehicular A model[22]

Delay [ns]	Relative Gain [dB]
0	0.0
310	-1.0
710	-9.0
1090	-10.0
1730	-15.0
2510	-20.0

Table 3.4: Multipath delay profile for ITU Vehicular B model[22]

Delay [ns]	Relative Gain [dB]
0	-2.5
300	0.0
8900	-12.8
12900	-10.0
17100	-25.2
20000	-16.0

3.2.1.4. Receive filter

The Receive Filter block, shown below in Figure 3.21, performs square-root raised cosine filtering on the I and Q sample streams with a filter that is matched to the transmit filter to maximize the in-band signal-to-noise ratio. The receive filter consists of filtering using the same square-root raised cosine filter that is used in the transmit filter and then downsampling by a factor of 8. The square-root raised cosine filter again has a roll-off factor of 0.22. Having the same parameters as the transmit filter, the receive filter works as a matched filter.

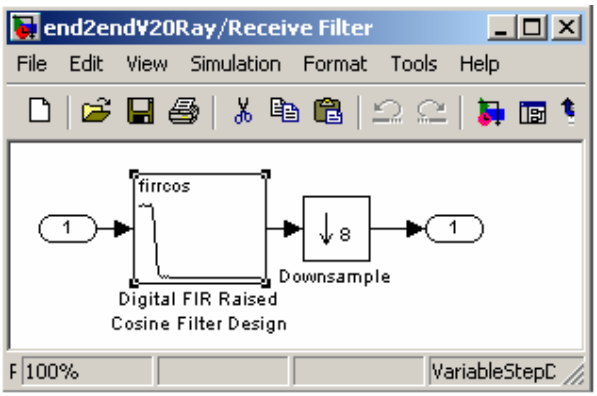

Figure 3.21: Receive filter block

3.2.1.5. Buffering

The signal is buffered into 80 chip blocks, so that the signal is processed 80 chips at a time, resulting in 480 blocks. This adds buffering delay to the system and as a result the first buffer frame is all zeros.

3.2.1.6. Correlator

The receiver detects the arrival time of the signal using a correlator. The mobile user receives the signal transmitted from the serving WCDMA base station through several paths with different propagation delays. The received signal, in addition to being corrupted by noise, is also distorted by the channel fading. The correlator detects the delayed path components.

The correlation between the received signal and locally generated complex Gold sequence is calculated. However, before performing this correlation, the locally

generated code is passed through the transmit and receive filters to compensate for the delay introduced by these filters.

Since both the received signal and the locally generated code are complex, the absolute value of their correlation is taken and the Maximum block finds the sample index where the correlation is a maximum. This sample index is sent to the workspace using the variable indexout for 480 frames.

This simulation uses the lag as the measure of the performance under the channel and noise conditions selected.

The simulation duration in this demo is set to process 10 ms. Because the frame duration in WCDMA is 10 ms, this simulation processes only 38400 chips of a frame. To convert a delay from samples to seconds, we simply multiply by the chip rate of 3.84 Mcps.

When correlating, we find only the first peak. We enter a value for the shadowing added path loss attenuated signal received signal power at this location into Multipath Rayleigh Fading block's gain field and find the multipath delays. Then, we enter another value for shadowing added path loss at this location into Multipath Rayleigh Fading block's gain field. We find the multipath as a result of this new value. We repeat this for 10 runs. Multipath components are resolvable at a resolution equal to the chip period. The positions of the peaks are fixed in time but the amplitudes are changing according to fast fading. In one instance, the first peak may be large in another instance the second, or third, and so on.

3.3. Geolocation System

In most geolocation systems, synchronization between base stations is a requirement. However, WCDMA is specified as an asynchronous network. Therefore, different measurements and techniques are necessary to locate a mobile station in such a network. In this section, we propose a time-difference-of-arrival technique, in which the mobile's serving base station sends a signal to the mobile, causing the mobile to respond to all three base stations at the same time. Each BS makes a measurement of

this round-trip propagation time. In addition, the MS makes a measurement of the signal arriving from each BS. This gives us a set of six measurements.

Let T_{propn} be the actual propagation time from base station n to the mobile station, where n = 1, 2, 3. Also, let $delayFW_n$ be the delay in the forward link from base station n to the mobile station and $delayRV_n$ be the delay in the reverse link from the mobile station to base station as a result of multipath propagation. t_{synchn} represents the synchronization offsets in the different base station clocks. t is the absolute time of transmission. The configuration is given below in Figure 3.22.

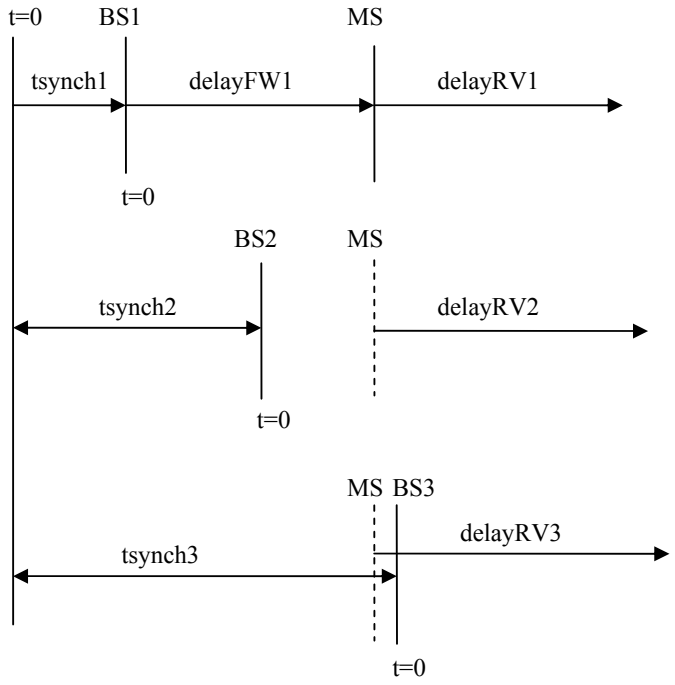

Figure 3.22: The timing relative to each BS

First, we ignore the effects of multipath propagation and obtain the equations needed to solve for the mobile position. In this case, the solution found is the actual mobile station location.

Figure 3.23 below illustrates the 3-base station geolocation system used for locating the mobile station. The points that are arranged in a triangular layout are the base station locations. The dot in between the BSs is the true MS location and the cross at the intersection of the hyperbolas is the estimated mobile location.

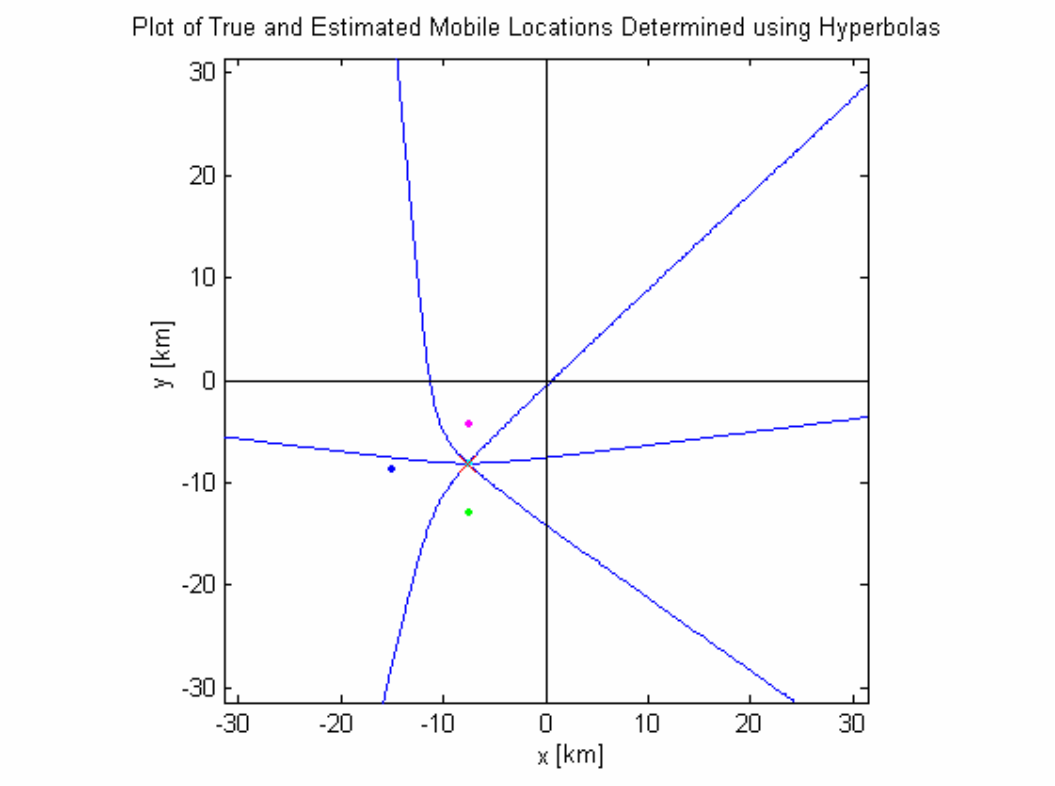

Figure 3.23: Geolocation system using three base stations and the TDOA method

We assume that the mobile station makes three measurements.

1. The MS measures BS1 at $t + t_{synch1} + T_{prop1} = const_1$. (3.4)
2. The MS measures BS2 at $t + t_{synch2} + T_{prop2} = const_2$. (3.5)
3. The MS measures BS3 at $t + t_{synch3} + T_{prop3} = const_3$. (3.6)

In addition, the BSs make one measurement each.

1. BS1 measures MS at $t + 2T_{prop1} = const_4$. (3.7)
2. BS2 measures MS at $t + (t_{synch1} - t_{synch2}) + T_{prop1} + T_{prop2} = const_5$. (3.8)
3. BS3 measures MS at $t + (t_{synch1} - t_{synch3}) + T_{prop1} + T_{prop3} = const_6$. (3.9)

Without loss of generality, we can set the absolute time of transmission, t, to 0. Then, using the measurements we have above, the true distances are

$$T_{prop1} = const_4 / 2 \tag{3.10}$$

Subtracting Equation 3.4 from Equation 3.5, we have

$$(T_{prop2} - T_{prop1}) + (t_{synch2} - t_{synch1}) = const_2 - const_1 \tag{3.11}$$

Subtracting Equation 3.4 from Equation 3.6, we have

$$(T_{prop3} - T_{prop1}) + (t_{synch3} - t_{synch1}) = const_3 - const_1 \tag{3.12}$$

Adding Equation 3.11 and Equation 3.8, we obtain

$$2T_{prop2} = (const_2 - const_1) + const_5 \tag{3.13}$$

We can solve for T_{prop2} using the equation above.

$$T_{prop2} = \frac{1}{2}\left[(const_2 - const_1) + const_5\right] \tag{3.14}$$

Adding Equation 3.12 and Equation 3.9, we obtain

$$2T_{prop3} = (const_3 - const_1) + const_6 \tag{3.15}$$

We can solve for T_{prop3} using the equation above.

$$T_{prop3} = \frac{1}{2}\left[(const_3 - const_1) + const_6\right] \tag{3.16}$$

We can also solve for t_{synch1}, t_{synch2}, and t_{synch3} is necessary.

$$t_{synch1} = const_1 - T_{prop1} \tag{3.17.a}$$

$$t_{synch2} = const_2 - T_{prop2} \tag{3.17.b}$$

$$t_{synch3} = const_3 - T_{prop3} \tag{3.17.c}$$

The equations above find the true mobile position when there is no delay due to multipath fading. In the case of a multipath fading channel,

1. T_{prop1} in Equation 3.4 is now actually $T_{prop1} + delayFW_1$.
2. T_{prop2} in Equation 3.5 is $T_{prop2} + delayFW_2$.
3. T_{prop3} in Equation 3.6 is $T_{prop3} + delayFW_3$.
4. $2T_{prop1}$ in Equation 3.7 is $(T_{prop1} + delayFW_1) + (T_{prop1} + delayRV_1)$.
5. In Equation 3.8, T_{prop1} is $T_{prop1} + delayFW_1$, T_{prop2} is $T_{prop2} + delayRV_2$.
6. In Equation 3.9, T_{prop1} is $T_{prop1} + delayFW_1$, T_{prop3} is $T_{prop3} + delayRV_3$.

In the above equations all three forward link delays and all three reverse link delays are independent. We plot the hyperbolas below, with the right-hand sides now being known constants.

$$(T_1 - T_2) = c_1 \tag{3.18.a}$$

$$(T_2 - T_3) = c_2 \tag{3.18.b}$$

$$(T_1 - T_3) = c_3 \tag{3.18.c}$$

We know the coordinates of the three base stations and these become the foci of the hyperbolas.

We calculate the differences between the distance measurements. For example,

$$diff_{13} = T_1 - T_3 \tag{3.19}$$

For the first calculation, we calculate the parameter a of the hyperbola. ‘a’ is the distance from the center to the vertex. ‘c’ is the distance form the center to the focus of the hyperbola. We calculate the x-and y-coordinates of the center of the hyperbola. We form the hyperbolas treating the locations of the base stations as the foci and the distance difference between them as ‘2a’.

Then we calculate the tilt angle. This angle specifies how much the hyperbola is rotated from its position on the x-axis.

If the time difference between the two base stations is zero, this means they are equidistant from the mobile station. In this case, the hyperbola is just a straight line described by

$$(y - yc_{13}) + \frac{1}{\tan(tilt)}(x - xc_{13}) = 0 \tag{3.20}$$

If the TDOA is not zero, we describe a u-v to x-y transformation, where the hyperbola lies on the v axis in u-v coordinates. The transformation is such that

$$u = x\cos\theta + y\sin\theta \tag{3.21.a}$$

$$v = y\cos\theta - x\sin\theta \tag{3.21.b}$$

Since hyperbolas have two branches, we look at the TDOA to decide which branch to use. For example, if diff13 is greater than zero, the MS is closer to BS3, and we use the equation.

$$\sqrt{(v - yc_{13uv} - c_{13})^2 + (u - xc_{13uv})^2} - \sqrt{(v - yc_{13uv} + c_{13})^2 + (u - xc_{13uv})^2} - 2a_{13} = 0 \tag{3.22}$$

On the other hand, if diff13 is less than zero, the MS is closer to BS1, and we use the equation.

$$\sqrt{(v - yc_{13uv} - c_{13})^2 + (u - xc_{13uv})^2} - \sqrt{(v - yc_{13uv} + c_{13})^2 + (u - xc_{13uv})^2} + 2a_{13} = 0 \tag{3.23}$$

The hyperbola for the BS2-BS3 pair and the hyperbola for the BS1-BS2 pair is found in the same way.

Solving only two equations of hyperbolas is sufficient to locate the mobile station. The module plots the hyperbolas and finds their intersection which is the location of the mobile.

The advantage of this geolocation system is that base station synchronization is not required. In the absence of multipath fading and noise, the location estimation is exact. This system also yields the exact synchronization differences of the base stations.

CHAPTER 4

RESULTS

This chapter describes the results obtained from the simulations described in the previous chapter.

4.1. Signal Spectra

We can trace the spectrum of the signal as it passes through the different blocks in the downlink model. Figure 4.1 below shows the spectrum of the pilot signal before spreading.

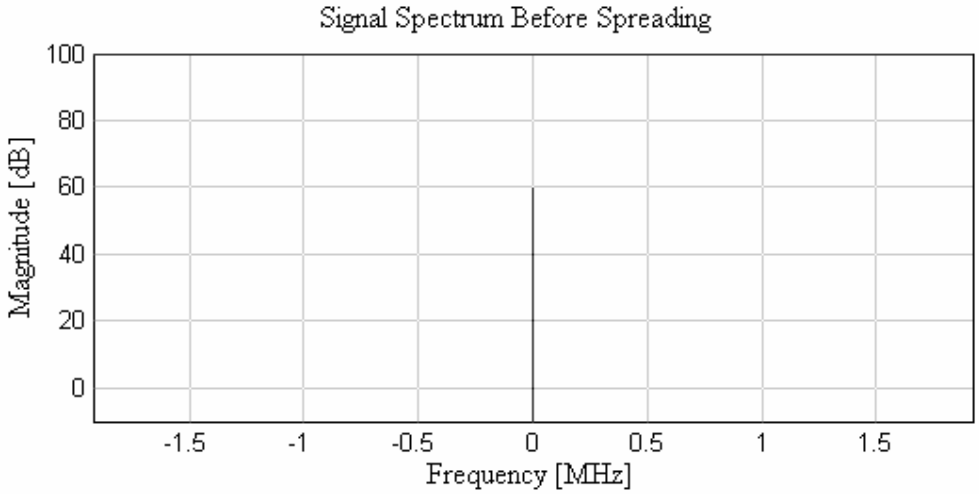

Figure 4.1: Spectrum of the pilot signal before spreading

Figure 4.2 below shows the spectrum of the pilot signal after complex spreading. This spread signal occupies a much larger bandwidth.

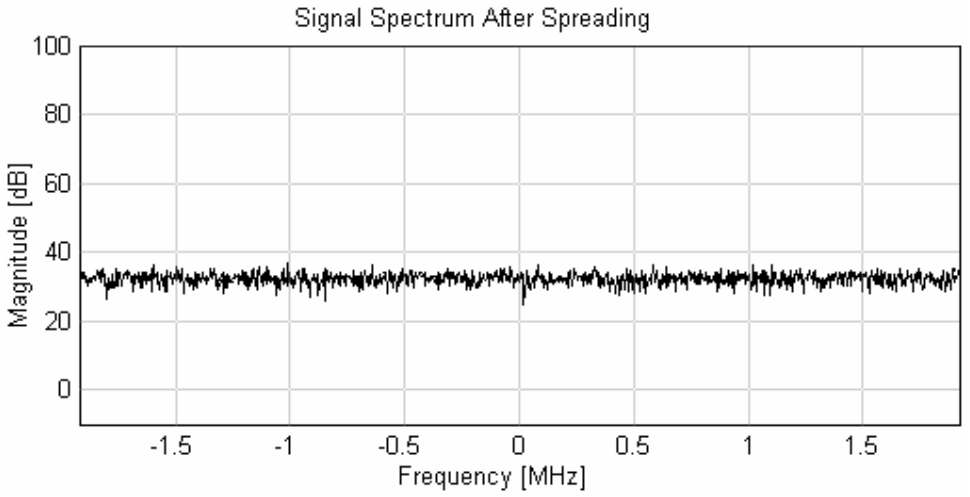

Figure 4.2: Spectrum of the spread signal after complex spreading

Figure 4.3 below shows the spectrum of the signal after it has been upsampled and shaped by the transmit filter. The maximum x-value in the graph below corresponds to half of the chip rate upsampled by 8. That is, $3.84MHz \times 8/2 = 15.36MHz$. We can see that the bandwidth is limited to 4.6848 MHz.

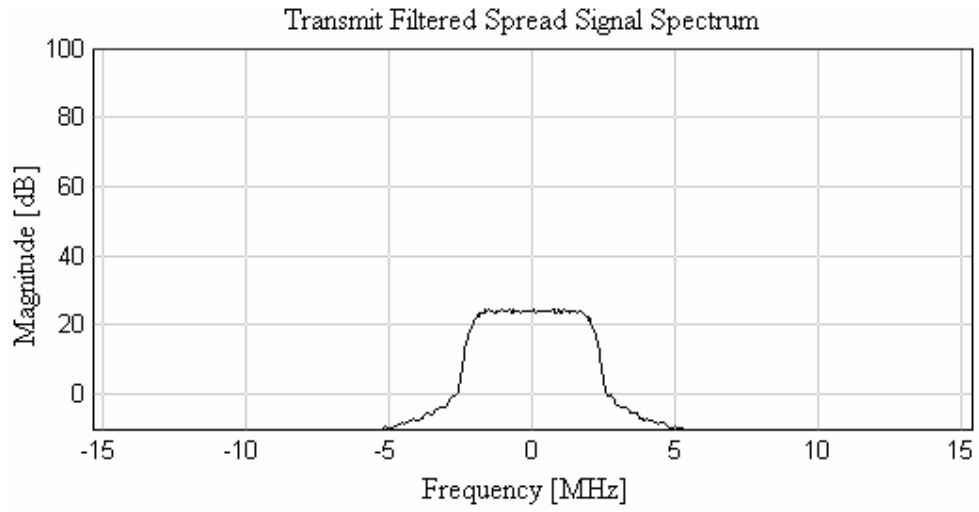

Figure 4.3: Spectrum of the spread signal after transmit filtering

Figure 4.4 below shows the spectrum of the signal after it passes through the Rayleigh fading and AWGN channel.

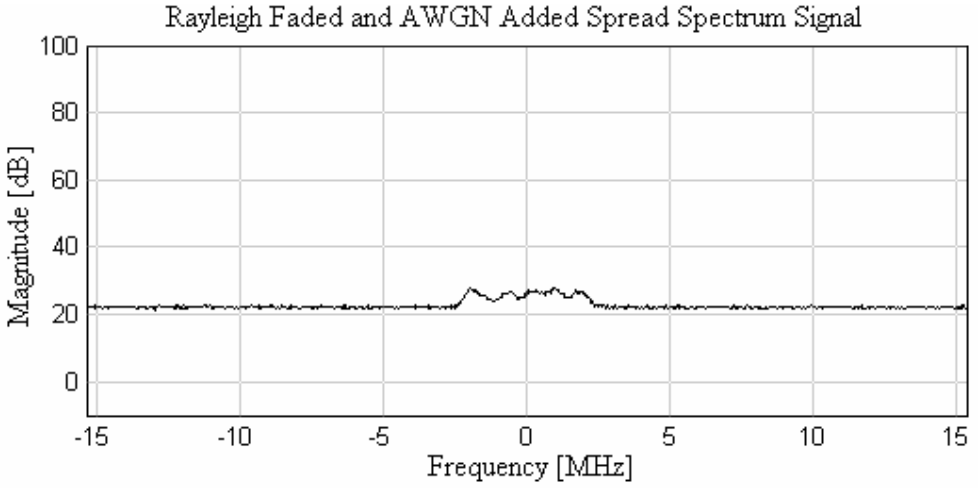

Figure 4.4: Spectrum of the signal after Rayleigh fading and AWGN channel

Figure 4.5 below shows the spectrum of the signal after it passes through the receive filter and is downsampled by 8.

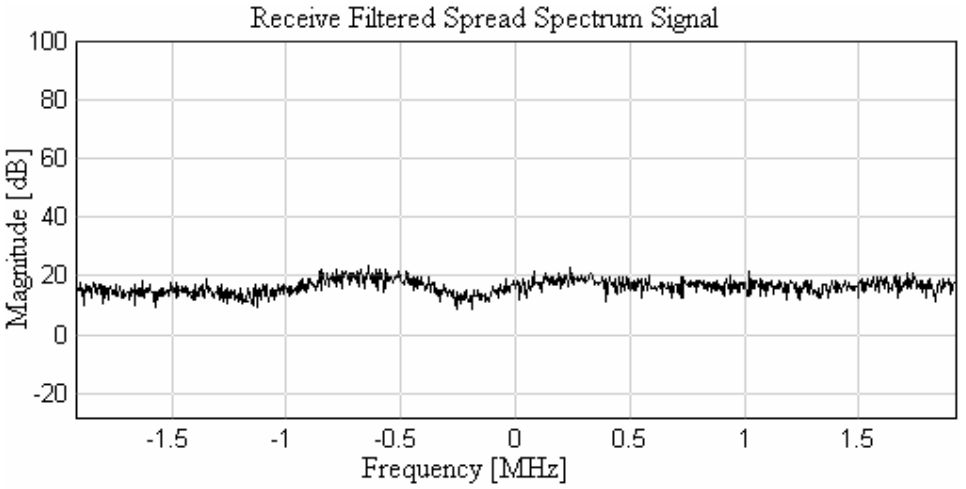

Figure 4.5: Spectrum of the receive filtered spread signal

The Scope block displays the in-phase and quadrature components of the spread waveform. The spread I and Q waveforms is shown below in Figure 4.6.

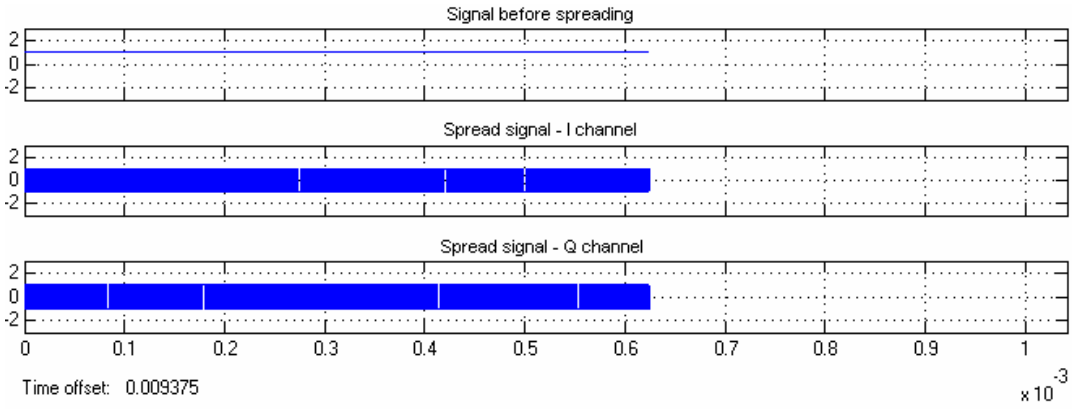

Figure 4.6: The pilot signal before spreading and the I&Q modulated channels

Taking a closer look at the waveforms yields Figure 4.7 below.

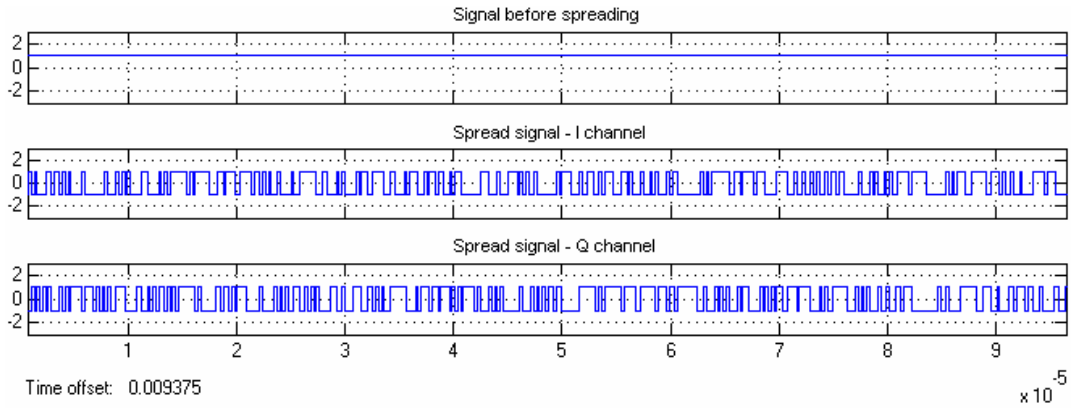

Figure 4.7: A closer look at the pilot signal before spreading and the modulated I&Q waveforms

Below in Figure 4.8, we can see the frame-based correlation.

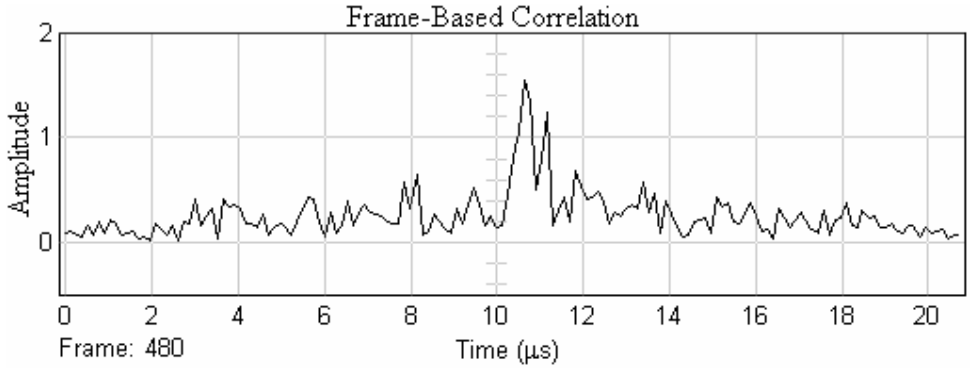

Figure 4.8: Frame-based correlation (frame size = 80)

4.2. Delays for Different Models

For the ATDMA Macro model, the multipath delays starting with the one at 380 ns, have all less than -10 dB relative gain. This causes the correlator to detect the peak at 0 ns most of the time.

As for the ITU Vehicular Model A, the peaks are detected mostly at 0 and at 1 chip offset corresponding to the multipath at 310 ns since this multipath has a relative gain quite close to the peak at 0, but the later multipaths are already attenuated by more than 8dB.

In the ITU Vehicular Model B, the relative gain of the peak at 300 ns, corresponding to 1 chip delay, is higher than the delay of the peak at 0. So, peaks are detected at mostly at 0 and at 1 chip offset, since the later multipaths are already attenuated by more than 12 dB.

The CODIT Macro model is by far the most interesting model, since it has many multipath components at delays close to each other and having similar relative gains. Peaks are detected at 0, 1, 2, 3, 4, 5, and 6 chip offsets. It is the model where a geolocation would be expected to be most erroneous. Below in Figure 4.9 is an example of delays obtained from this model.

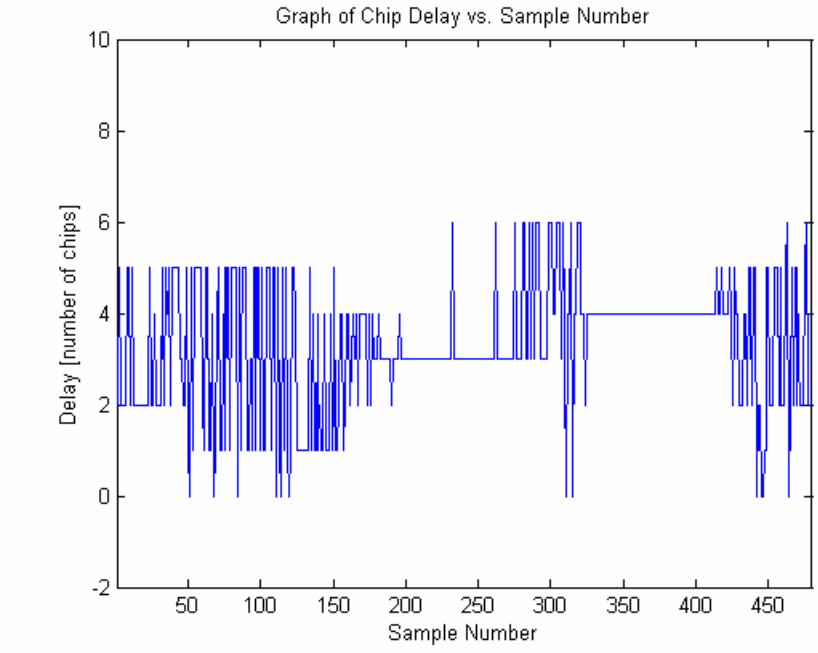

Figure 4.9: Chip delay versus sample number for CODIT Macro model

4.3. COST-231 Suburban Model

The function interfatpointsuburban.m is executed 10 times to find the path loss attenuated and shadow faded received signal strengths below in Table 4.1.

Table 4.1: The received signal strengths at MS location for 10 runs using the COST-231 suburban model

	Signal BS1 [dB]	Signal BS2 [dB]	Signal BS3 [dB]
Run 1	-173.6546	-155.6646	-169.0243
Run 2	-172.2329	-156.6556	-163.4622
Run 3	-163.8338	-153.2657	-153.0697
Run 4	-168.8469	-163.8787	-157.7564
Run 5	-172.3820	-155.4509	-150.8999
Run 6	-161.7865	-158.3485	-163.1803
Run 7	-151.5169	-154.8789	-157.5286
Run 8	-163.9884	-160.4763	-172.0266
Run 9	-177.1649	-162.7438	-160.0410
Run 10	-166.6834	-168.8776	-157.1118

The received signal strengths above are used in the Rayleigh fading model.

4.3.1. CODIT Channel Model

For the CODIT Channel Model, the PN offsets are stored in the variable, indexout, resulting in a sample size of 102. The MS location is estimated for 100 of these sample offsets. These locations are stored in the matrix files cdtrun1solx12.mat using the variable solx12 and cdtrun1soly12.mat using the variable soly12. These correspond to the x- and y-coordinates of the estimates, respectively. The error is estimated using

$$error = \sqrt{(solx12 - xMS)^2 + (soly12 - yMS)^2} \tag{4.1}$$

where xMS and yMS are the true mobile location coordinates.

Below in Figure 4.10, we see a graph of this error.

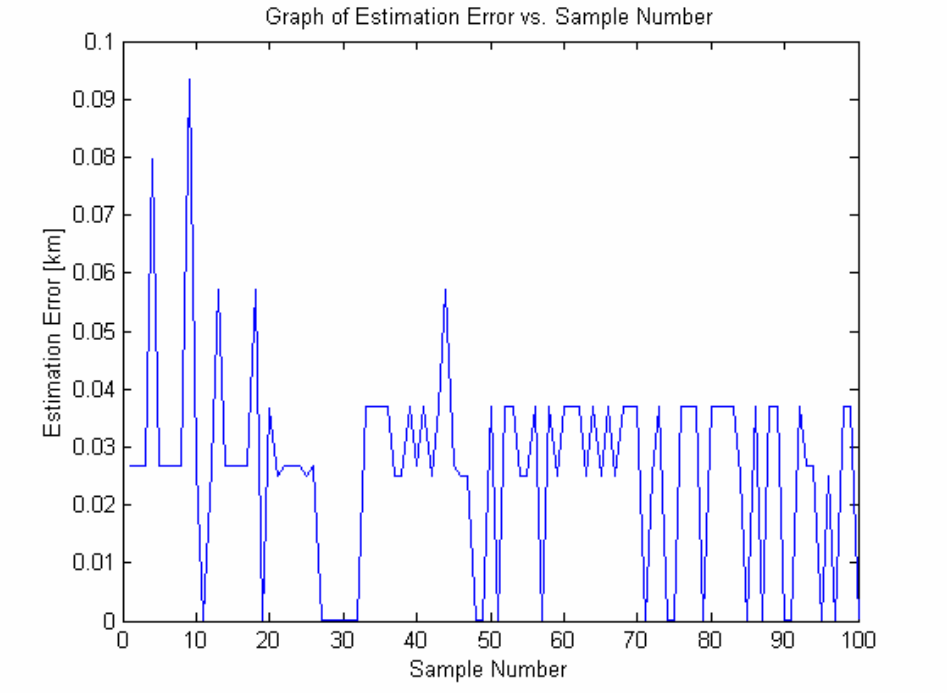

Figure 4.10: Estimation error versus sample number

Below in Figure 4.11, we see the cumulative distribution function of this error.

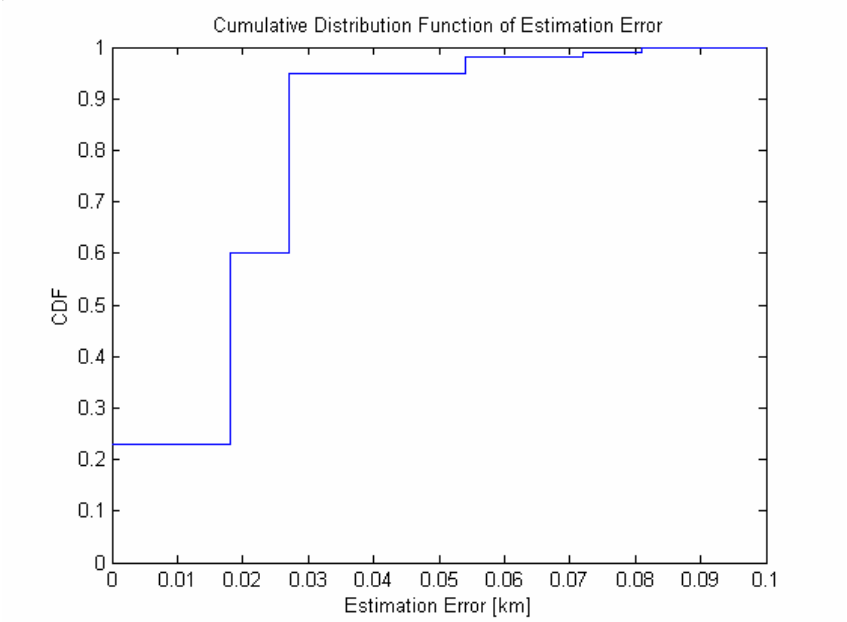

Figure 4.11: CDF of estimation error for suburban CODIT

Figure 4.11 shows that the error is within 30 m, 90% of the time.

4.3.2. ATDMA Channel Model

The error estimation is similar to Section 4.3.1 above. We obtain the cumulative distribution function of this error shown below in Figure 4.12.

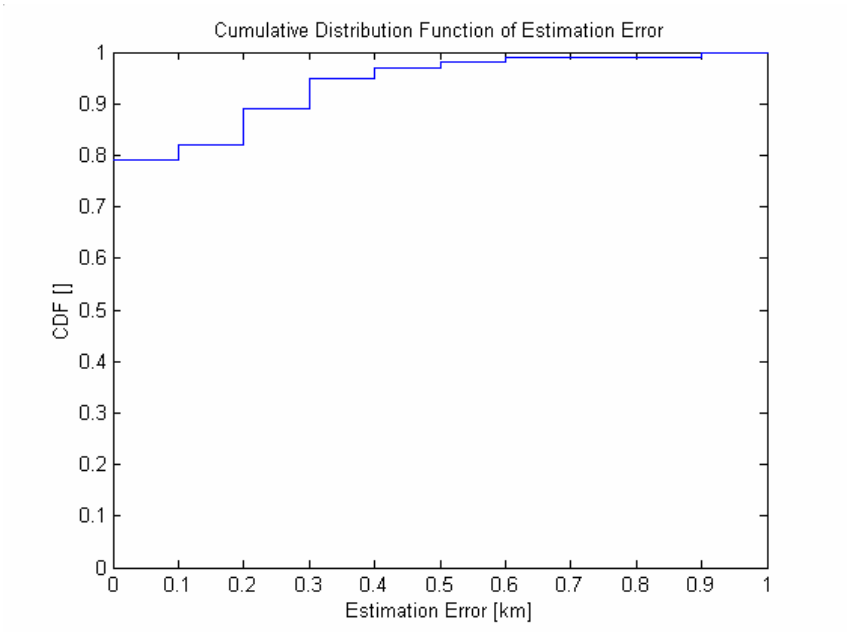

Figure 4.12: CDF of estimation error for suburban ATDMA

Figure 4.12 shows that the error is within 20 m, 90% of the time.

4.3.3. ITU Vehicular A Channel Model

The error estimation is similar to Section 4.3.1 above. We obtain the cumulative distribution function of this error shown below in Figure 4.13.

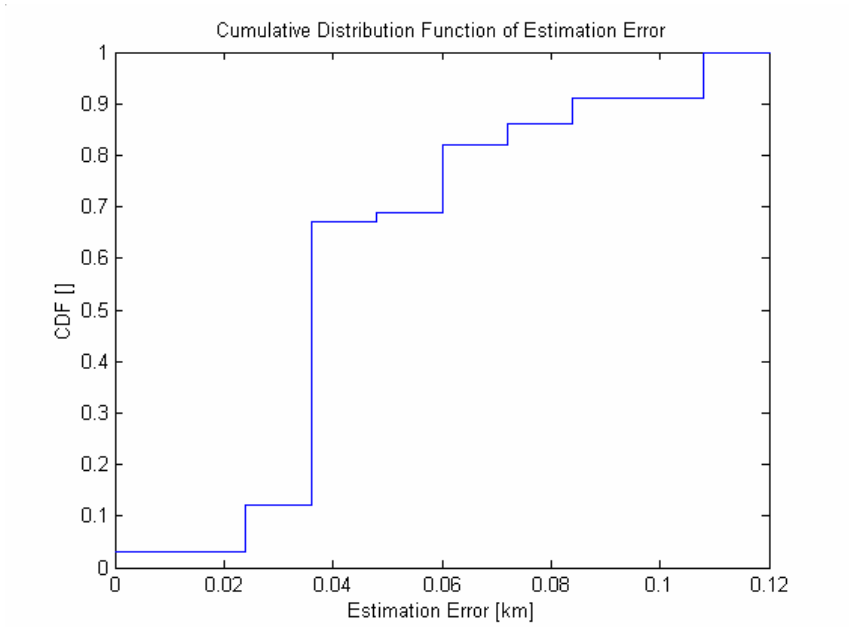

Figure 4.13: CDF of estimation error for suburban ITU Vehicular A

Figure 4.13 shows that the error is within 85 m, 90% of the time.

4.3.4. ITU Vehicular B Channel Model

The error estimation is similar to Section 4.3.1 above. We obtain the cumulative distribution function of this error shown below in Figure 4.14.

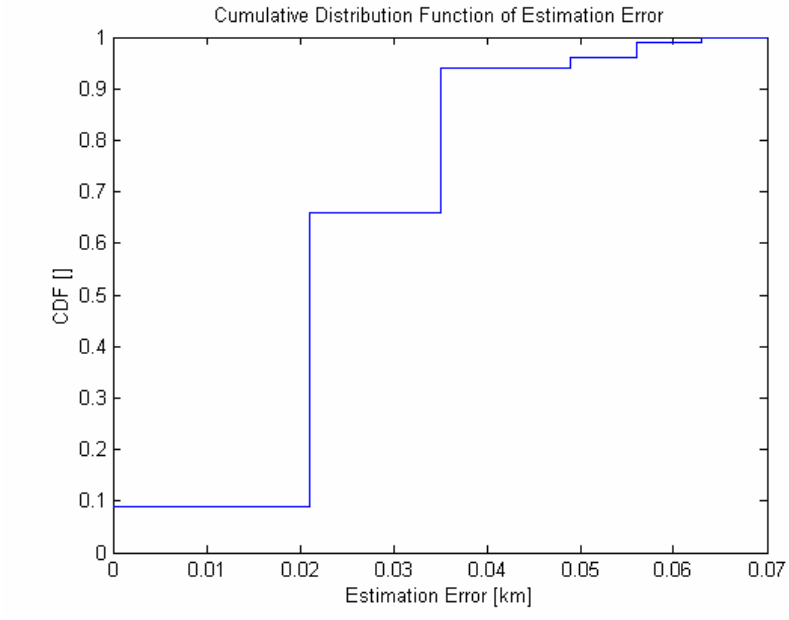

Figure 4.14: CDF of estimation error for suburban ITU Vehicular B

Figure 4.14 shows that the error is within 35 m, 90% of the time.

4.4. COST-231 Urban Model

The function interfatpointurban.m is executed 10 times to find the path loss attenuated and shadow faded received signal strengths below in Table 4.2.

Table 4.4: The received signal strengths at MS location for 10 runs using the COST-231 urban model

	Signal BS1 [dB]	Signal BS2[dB]	Signal BS3 [dB]
Run 1	-171.6829	-168.5706	-170.5151
Run 2	-180.8656	-155.8021	-158.2442
Run 3	-168.6042	-168.9299	-158.9435
Run 4	-179.4701	-167.5081	-159.9345
Run 5	-173.9080	-159.1090	-156.5446
Run 6	-163.5156	-164.1222	-167.1575
Run 7	-168.2022	-167.6572	-158.7297
Run 8	-161.3458	-157.0617	-161.6274
Run 9	-173.6261	-146.7921	-158.1578
Run 10	-167.9744	-159.2637	-163.7552

4.4.1. CODIT Channel Model

The error estimation is similar to Section 4.3.1 above. We obtain the cumulative distribution function of this error shown below in Figure 4.15.

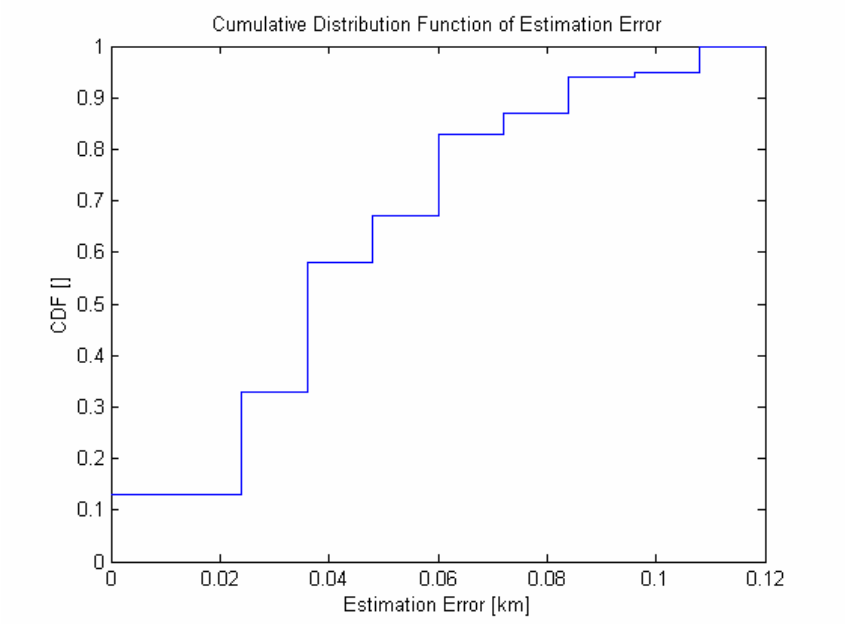

Figure 4.15: CDF of estimation error for urban CODIT

Figure 4.15 shows that the error is within 85 m, 90% of the time.

4.4.2. ATDMA Channel Model

The error estimation is similar to Section 4.3.1 above. We obtain the cumulative distribution function of this error shown below in Figure 4.16.

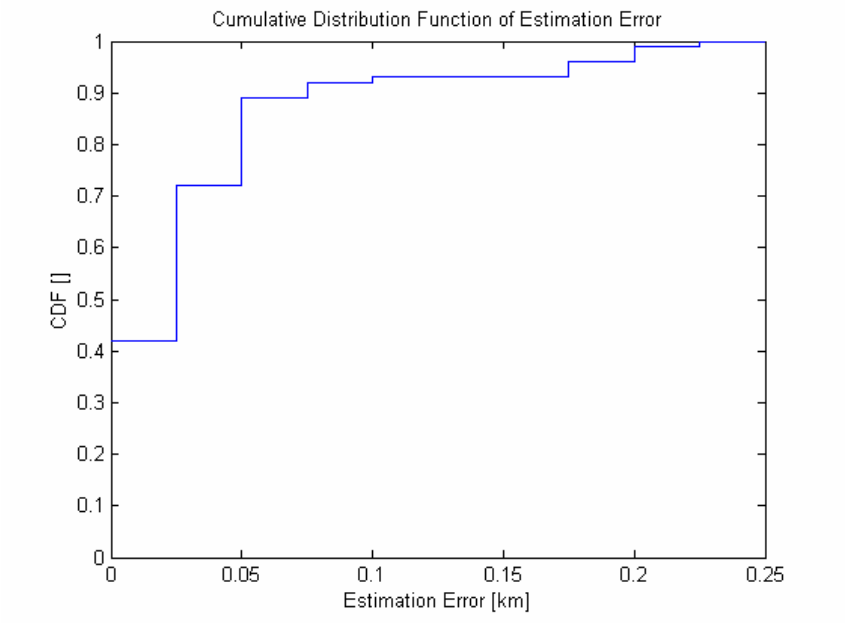

Figure 4.16: CDF of estimation error for urban ATDMA

Figure 4.16 shows that the error is within 75 m, 90% of the time.

4.4.3. ITU Vehicular A Channel Model

The error estimation is similar to Section 4.3.1 above. We obtain the cumulative distribution function of this error shown below in Figure 4.17.

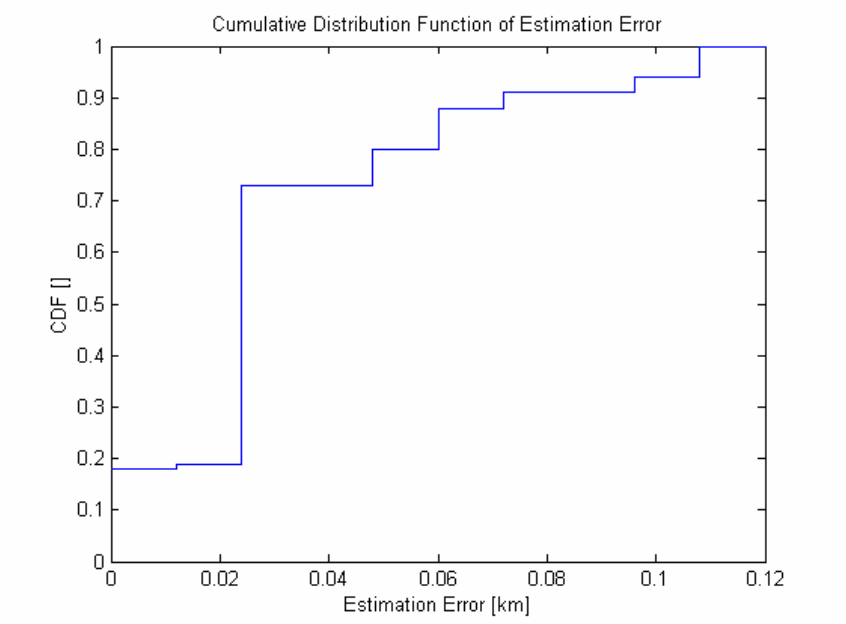

Figure 4.17: CDF of estimation error for urban ITU Vehicular A

Figure 4.17 shows that the error is within 70 m, 90% of the time.

4.4.4. ITU Vehicular B Model

The error estimation is similar to Section 4.3.1 above. We obtain the cumulative distribution function of this error shown below in Figure 4.18.

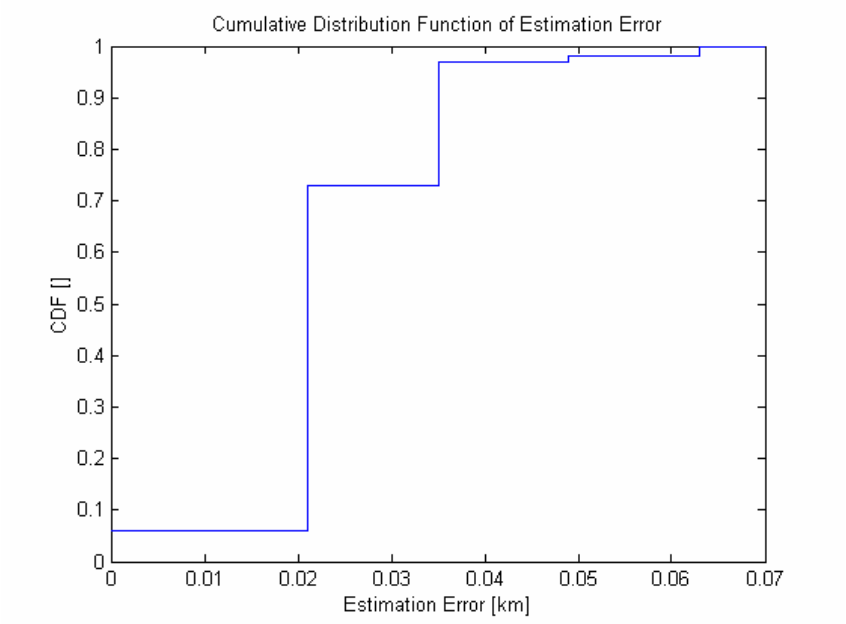

Figure 4.18: CDF of estimation error for urban ITU Vehicular B

Figure 4.18 shows that the error is within 35 m, 90% of the time.

4.5. COST-231 Rural Model

The function interfatpointrural.m is executed 10 times to find the path loss attenuated and shadow faded received signal strengths below in Table 4.3.

Table 4.7: The received signal strengths at MS for 10 runs using COST-231 rural model

	Signal BS1 [dB]	Signal BS2[dB]	Signal BS3 [dB]
Run 1	-147.0008	-136.9684	-130.5510
Run 2	-135.0152	-126.4870	-136.6848
Run 3	-132.0860	-123.0129	-137.8564
Run 4	-141.3815	-125.8941	-98.0028
Run 5	-111.8883	-120.2477	-109.1759
Run 6	-124.9310	-139.0041	-119.6150
Run 7	-125.2105	-117.7585	-118.3176
Run 8	-125.7683	-128.8570	-128.1422
Run 9	-135.9192	-130.5091	-126.2617
Run 10	-136.9713	-131.8649	-112.1282

4.5.1. CODIT Channel Model

The error estimation is similar to Section 4.3.1 above. We obtain the cumulative distribution function of this error shown below in Figure 4.19.

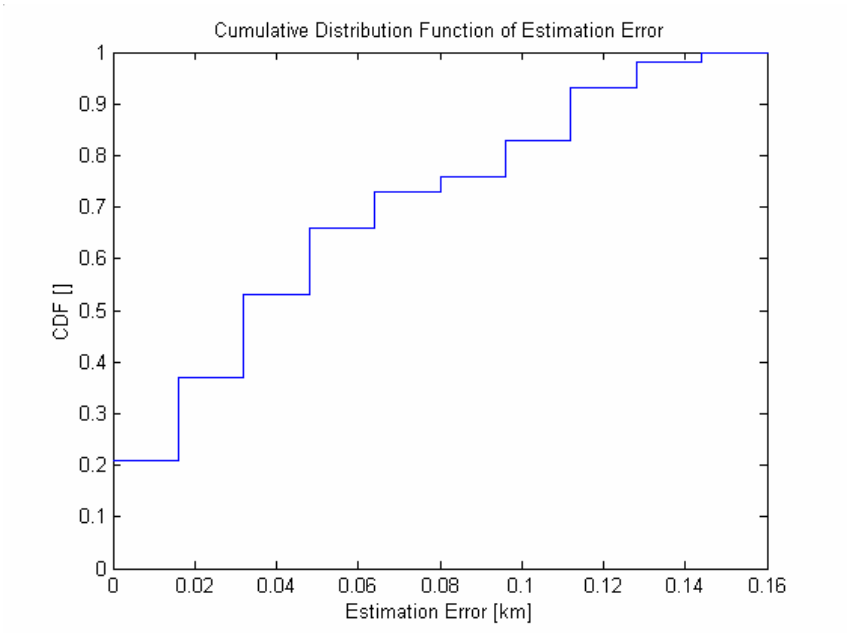

Figure 4.19: CDF of estimation error for rural CODIT

Figure 4.19 shows that the error is within 110 m, 90% of the time.

4.5.2. ATDMA Channel Model

The error estimation is similar to Section 4.3.1 above. We obtain the cumulative distribution function of this error shown below in Figure 4.20.

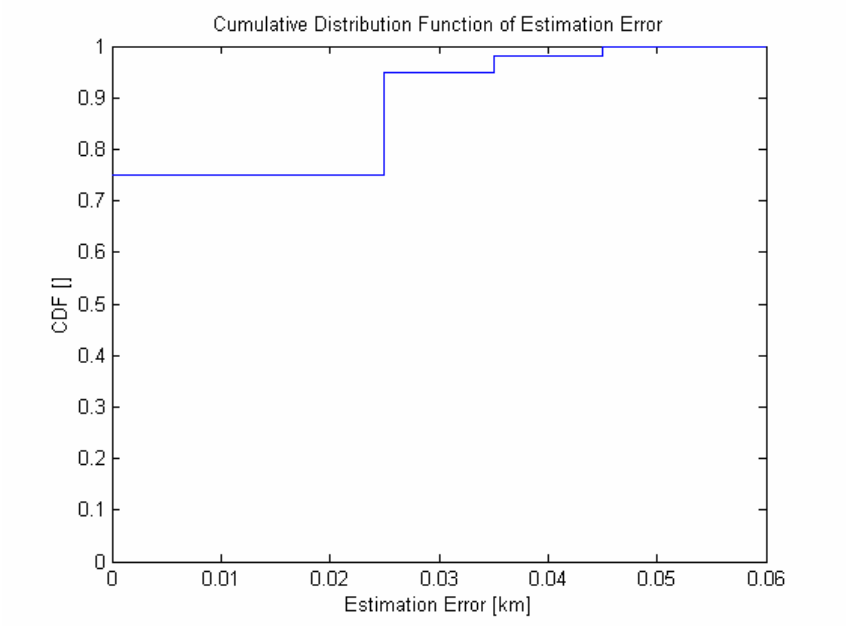

Figure 4.20: CDF of estimation error for rural ATDMA

Figure 4.20 shows that the error is within 25 m, 90% of the time.

4.5.3. ITU Vehicular A Model

The error estimation is similar to Section 4.3.1 above. We obtain the cumulative distribution function of this error shown below in Figure 4.21.

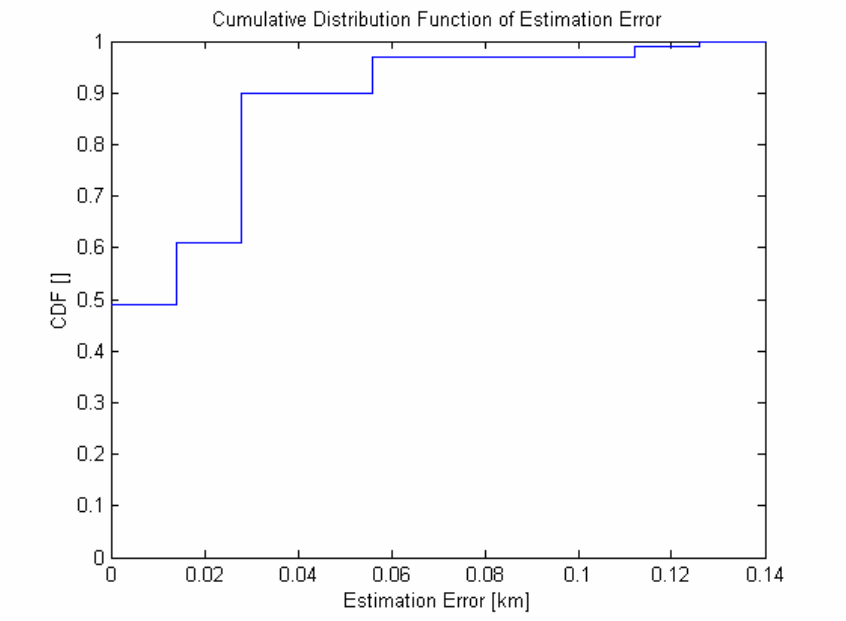

Figure 4.21: CDF of estimation error for rural ITU Vehicular A

Figure 4.21 shows that the error is within 50 m, 90% of the time.

4.5.4. ITU Vehicular B Model

The error estimation is similar to Section 4.3.1 above. We obtain the cumulative distribution function of this error shown below in Figure 4.22.

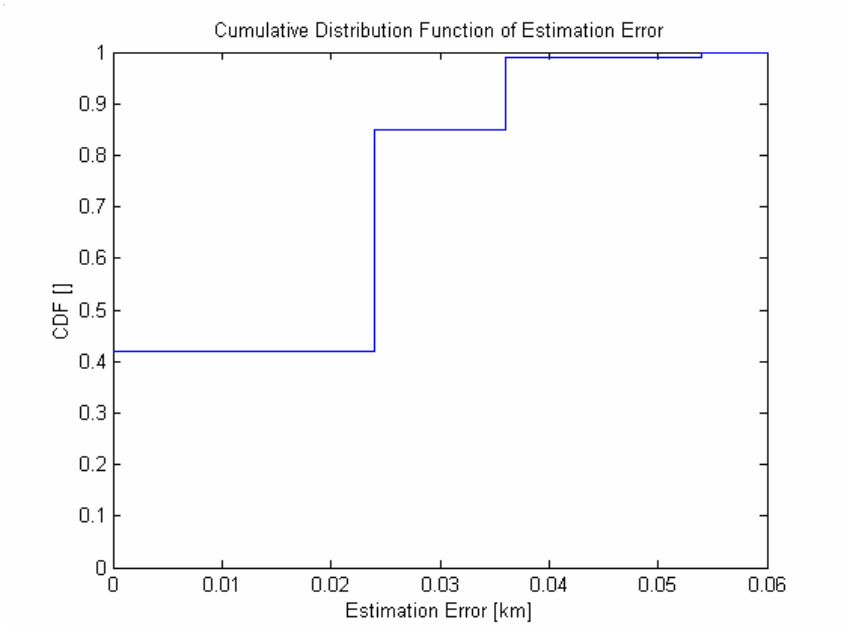

Figure 4.22: CDF of estimation error for rural ITU Vehicular B

Figure 4.22 shows that the error is within 35 m, 90% of the time.

4.6. Estimation Error Using 40960-Chip Complex Spreading

For comparison, the former WCDMA specification using 40960-chip complex Gold code spreading (with a shift of 3584 chips instead of the 131072 chips in the current specification) is also simulated for the COST-231 suburban model using the CODIT channel. The error estimation is similar to Section 4.3.1 above. The cumulative distribution function of this error is shown below in Figure 4.23.

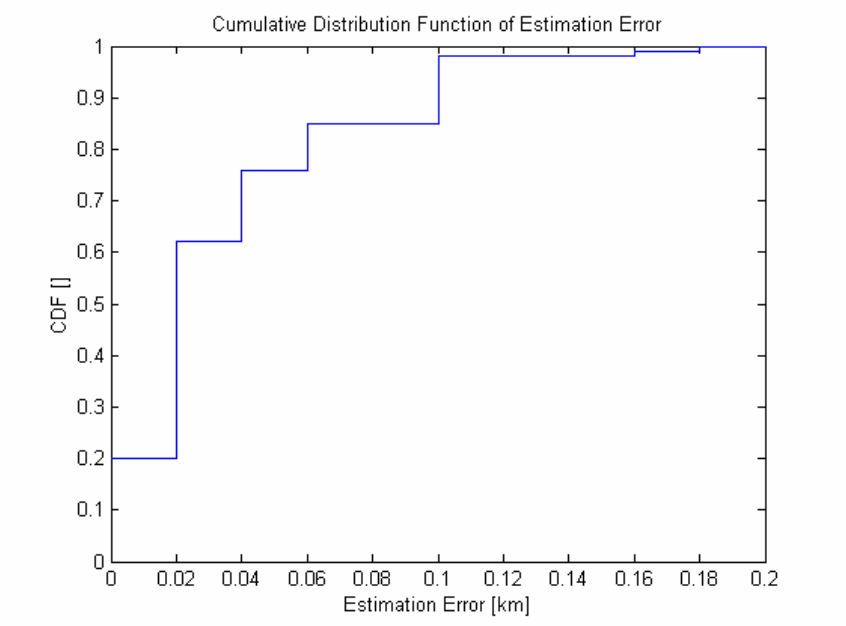

Figure 4.23: CDF of estimation error for suburban CODIT 40960

Figure 4.23 shows that the error is within 100 m, 90% of the time.

CHAPTER 5

CONCLUSION

We simulated a wireless geolocation system for use in a WCDMA environment. In such a system, the multipath delays have a significant effect on the mobile location estimate.

First, the path loss, shadowing, and fading models were analyzed for a 19-cell 3-sector topology. Then, using the WCDMA system specifications in the end-to-end model, the pilot signal was spread using 38400-chip complex Gold spreading and shaped using a transmit filter. The effects of multipath fading and noise were added. The multipath fading depends on the shadowing added path loss attenuated received signal strength.

At the receiver, the received signal was passed through a receive filter and correlated with the mobile station's locally generated Gold code. The peaks of the correlator determine which multipath delay is taken to be the distance from the base station. The geolocation system estimates the mobile location using the delay added propagation times. The time-difference-of-arrival approach was employed for forming an estimate of the mobile station using three base stations.

Performance measures for a geolocation system include accuracy. We investigated the error made in the location estimates of mobile station location as a result of multipath fading. The 90% estimation errors are summarized below in Table 5.1. The estimation errors are less than the numbers listed in the table 90% of the time.

Table 5.1: 90% estimation errors for various environments and channels

Estimation Error [m]				
	CODIT	ATDMA	ITU Vehicular A	ITU Vehicular B
Suburban	30	20	85	35
Urban	85	75	70	35
Rural	110	25	50	35

These errors are acceptable, considering that one chip time corresponds to 78 m. Also, for comparison, the former WCDMA specification of 40960-chip complex spreading was evaluated and in this case the error was found to be 100 m for the COST-231 suburban model using the CODIT Macro Channel. In this case, one chip time corresponds to 73 m.

However, this error is restricted to the COST-231 path loss model and a shadowing with standard deviation of 8 dB. Changing the path loss model and the shadowing would result in a change in the error estimate. The COST-231 model may be more idealistic than actual field measurements of a WCDMA network. Making the necessary changes to the end-to-end system presents no problems. The spreading chip rate can also be changed if necessary.

This simulation system can thus be used to evaluate the performance of a WCDMA geolocation network with different parameters. Path loss and shadowing models are useful for network planning and the multipath delay profile is necessary for communications system design.

5.1. Future Work

The correlator can be changed to work using a preset threshold and identify the earliest peak that is higher than this threshold, instead of picking up the highest peak. The simulator can further be improved by using statistical channel models based on measured data obtained from an actual WCDMA network.

The algorithms can be tested under real world conditions. We have simulated the model with an ideal base station configuration. This model can be evaluated in a non-ideal base station arrangement, since real networks do not use the ideal hexagonal

layout. In all the simulations, we have assumed that the algorithm can detect the moving mobile's position fast enough. Yet, the position estimation is stationary. The algorithms can be changed to track a moving mobile in real time.

REFERENCES

[1] S. Y. Willassen, "A method for implementing mobile station location in GSM," MS thesis, Norwegian Univ. of Tech. and Sci., Dept. of Telematics, Philadelphia, 1998.

[2] J. M. Zagami, S. A. Parl, J. J. Bussgang, and K.D. Melillo, "Providing universal location services using a wireless E911 location network," *IEEE Comm. Mag.*, pp. 66-71, Apr. 1998.

[3] M. O. Sunay and I. Tekin, "Mobile location tracking for IS-95 networks using the forward link time difference of arrival and its application to zone-based billing," in *Proc. IEEE Glob. Telecom. Conf.*, Dec. 5-9, 1999.

[4] J. H. Reed, K. J. Krizman, B. D. Woerner, and T. S. Rappaport, "An overview of the challenges and progress in meeting the E-911 requirement for location service," *IEEE Comm. Mag.*, pp. 30-37, Apr. 1998.

[5] Technical Specification Group Radio Access Network, "CPICH for acquisition purposes," 3GPP, TSGR 4(99)368, Jun.1999.

[6] G. Wade, *Coding Techniques*. New York: Palgrave, 2000.

[7] J. Korhonen, *Introduction to 3G Mobile Communications*. Boston: Artech House, 2001.

[8] ETSI , "High-level requirements relevant for the definition of the UMTS terrestrial radio access (UTRA) concept," Technical Report TR 101 398 v.3.0.1, Oct. 1998.

[9] E. Saygun, *Course Notes for EE 584, Special Topics in Telecommunications I*: *GSM*, Sabanci University, Fall semester, 2001.

[10] B. Sklar, "Rayleigh fading channels in mobile digital communication systems part I: characterization," *IEEE Comm. Mag.*, vol. 35, no. 9, pp.136-156, Sept. 1997.

[11] I. Tekin, *Course Notes for EE 556*, *Antennas and Propagation*, Sabanci University, Spring semester, 2001.

[12] K. Fall and K. Varadhan, *ns Manual*, ch.17, p.165.

[13] T. S. Rappaport, *Wireless Communications Principles & Practice*. Upper Saddle River: Prentice Hall, 1996.

[14] G. S. Prabhu and P. M. Shankar, "Simulation of flat-fading using MATLAB for classroom instruction," Drexel Uni., Dept. of Electrical and Computer Eng., Philadelphia, 1998.

[15] G. L. Stuber and J. J. Caffery, Jr., “Chapter 24 radiolocation techniques.” In J. D. Gibson and E. M. Gibson, eds. *The Mobile Communications Handbook*, 2nd ed. Boca Raton: CRC, 1999.

[16] J. J. Caffery, Jr. and G. L. Stuber, “Overview of radiolocation in CDMA cellular systems,” *IEEE Comm*. *Mag*., pp. 38-45, Apr. 1998.

[17] Technical Specification Group Radio Access Network, “Spreading and modulation (FDD) (Release 5),” 3GPP, Technical Specification 3G TS 25.213 v. 5.0.0, Mar.2002.

[19] *CDMA Reference Blockset User’s Guide*. The Mathworks, Inc., 2001.

[20] Technical Specification Group Radio Access Networks, “UE Radio transmission and reception (FDD) (Release 5),” 3GPP, Technical Specification 3G TS 25.101 v. 5.3.0, Jun. 2002.

[21] T. Ojanpera and R. Prasad, *Wideband CDMA for Third Generation Mobile Communications*. Boston: Artech House, 1998.

[22] TSG-RAN Working Group 1, “Further results on CPICH interference cancellation as a means for increasing DL capacity,” 3GPP, Technical Specification TSGR1-01-0030.

REFERENCES

[1] S. Y. Willassen, "A method for implementing mobile station location in GSM," MS thesis, Norwegian Univ. of Tech. and Sci., Dept. of Telematics, Philadelphia, 1998.

[2] J. M. Zagami, S. A. Parl, J. J. Bussgang, and K.D. Melillo, "Providing universal location services using a wireless E911 location network," *IEEE Comm. Mag.*, pp. 66-71, Apr. 1998.

[3] M. O. Sunay and I. Tekin, "Mobile location tracking for IS-95 networks using the forward link time difference of arrival and its application to zone-based billing," in *Proc. IEEE Glob. Telecom. Conf.*, Dec. 5-9, 1999.

[4] J. H. Reed, K. J. Krizman, B. D. Woerner, and T. S. Rappaport, "An overview of the challenges and progress in meeting the E-911 requirement for location service," *IEEE Comm. Mag.*, pp. 30-37, Apr. 1998.

[5] Technical Specification Group Radio Access Network, "CPICH for acquisition purposes," 3GPP, TSGR 4(99)368, Jun.1999.

[6] G. Wade, *Coding Techniques*. New York: Palgrave, 2000.

[7] J. Korhonen, *Introduction to 3G Mobile Communications*. Boston: Artech House, 2001.

[8] ETSI , "High-level requirements relevant for the definition of the UMTS terrestrial radio access (UTRA) concept," Technical Report TR 101 398 v.3.0.1, Oct. 1998.

[9] E. Saygun, *Course Notes for EE 584, Special Topics in Telecommunications I*: *GSM*, Sabanci University, Fall semester, 2001.

[10] B. Sklar, "Rayleigh fading channels in mobile digital communication systems part I: characterization," *IEEE Comm. Mag.*, vol. 35, no. 9, pp.136-156, Sept. 1997.

[11] I. Tekin, *Course Notes for EE 556*, *Antennas and Propagation*, Sabanci University, Spring semester, 2001.

[12] K. Fall and K. Varadhan, *ns Manual*, ch.17, p.165.

[13] T. S. Rappaport, *Wireless Communications Principles & Practice*. Upper Saddle River: Prentice Hall, 1996.

[14] G. S. Prabhu and P. M. Shankar, "Simulation of flat-fading using MATLAB for classroom instruction," Drexel Uni., Dept. of Electrical and Computer Eng., Philadelphia, 1998.

[15] G. L. Stuber and J. J. Caffery, Jr., “Chapter 24 radiolocation techniques.” In J. D. Gibson and E. M. Gibson, eds. *The Mobile Communications Handbook*, 2nd ed. Boca Raton: CRC, 1999.

[16] J. J. Caffery, Jr. and G. L. Stuber, “Overview of radiolocation in CDMA cellular systems,” *IEEE Comm*. *Mag*., pp. 38-45, Apr. 1998.

[17] Technical Specification Group Radio Access Network, “Spreading and modulation (FDD) (Release 5),” 3GPP, Technical Specification 3G TS 25.213 v. 5.0.0, Mar.2002.

[19] *CDMA Reference Blockset User’s Guide*. The Mathworks, Inc., 2001.

[20] Technical Specification Group Radio Access Networks, “UE Radio transmission and reception (FDD) (Release 5),” 3GPP, Technical Specification 3G TS 25.101 v. 5.3.0, Jun. 2002.

[21] T. Ojanpera and R. Prasad, *Wideband CDMA for Third Generation Mobile Communications*. Boston: Artech House, 1998.

[22] TSG-RAN Working Group 1, “Further results on CPICH interference cancellation as a means for increasing DL capacity,” 3GPP, Technical Specification TSGR1-01-0030.